THE EFFECTS OF EXTRACELLULAR VESICLE-ASSOCIATED KINASES ON HIV-1 PATHOGENESIS

by

Gifty A. Mensah

A Dissertation
Submitted to the
Graduate Faculty
of
George Mason University
in Partial Fulfillment of
The Requirements for the Degree
of
Doctor of Philosophy
Biosciences

Committee:

_____	Dr. Fatah Kashanchi, Committee Chair
_____	Dr. Lance Liotta, Committee Member
_____	Dr. Ramin Hakami, Committee Member
_____	Dr. Sergei Nekhai, Committee Member
_____	Dr. Iosif Vaisman, Director, School of Systems Biology
_____	Dr. Donna M. Fox, Associate Dean, Office of Student Affairs & Special Programs, College of Science
_____	Dr. Fernando R. Miralles-Wilhelm Dean, College of Science
Date: _____	Summer Semester 2022 George Mason University Fairfax, VA

The Effects of Extracellular Vesicle-Associated Kinases on HIV-1 Pathogenesis

A Dissertation submitted in partial fulfillment of the requirements for the degree of Doctor of Philosophy at George Mason University

by

Gifty A. Mensah
Master of Science
George Mason University, 2019

Director: Fatah Kashanchi, Professor
George Mason University

Summer Semester 2022
George Mason University
Fairfax, VA

DEDICATION

This is dedicated to my loving husband, Derrick, and my wonderful baby, Sky.

ACKNOWLEDGEMENTS

I would like to thank all the many people that supported me throughout this journey and made this happen. This includes my PI, Dr. Fatah Kashanchi; my graduate committee members; my fellow lab members namely Pooja, Yuriy, Anastasia, James, Emre, and Zach; my former mentor, Dr. Alex Barclay; collaborators; and the people at the GMU provost office especially Dr. Laurence Bray and Ms. Pallavi Rai Gullo. I would also like to give a special thanks to my relatives above all my husband, Derrick, for all his unwavering support and care, as well as my parents and siblings.

TABLE OF CONTENTS

LIST OF TABLES

Table **Page**

LIST OF FIGURES

Figure **Page**

LIST OF ABBREVIATIONS

Extracellular Vesicle ..... EV
Human Immunodeficiency Virus-1 ..... HIV-1
Acquired Immunodeficiency Syndrome ..... AIDS
Combined Antiretroviral Therapy ..... cART
HIV-1 Associated Neurological Disorder ..... HAND
Intercellular Adhesion Molecule-1 ..... ICAM-1
Differential Ultracentrifugation ..... DUC
Whole Cell Extract ..... WCE
Long Terminal Repeat ..... LTR
Peripheral Blood Mononuclear Cell ..... PBMC
Nanotrap ..... NT
Cellular Src Kinase ..... c-Src
Src Family of Kinases ..... SFKs
Phosphoinositide 3-Kinase PI3K
Mammalian Target of Rapamycin ..... mTOR
Steroid Receptor Coactivator 1 ..... SRC-1
Epidermal Growth Factor ..... EGFR
Jun N-terminal protein Kinase ..... JNK
Cyclin-Dependent Kinase 10 ..... CDK10
Glycogen Synthase Kinase-3 beta GSK3β
Cerebrospinal Fluid ..... CSF
Short HIV-1 Transcript ..... ST
Multivesicular Bodies ..... MVBs
Microvesicle ..... MV
Receptor Tyrosine Kinase ..... RTK
Signal Transducer and Activator of Transcription 3 ..... STAT3
Transactivation Response ..... TAR
Fetal Bovine Serum ..... FBS
Phosphate Saline ..... PBS
Reverse Transcriptase ..... RT
Polymerase Chain Reaction ..... PCR
Quantified Polymerase Chain Reaction ..... qPCR
RNA Polymerase II ..... Pol II
Small Interfering RNA ..... siRNA
Human T-cell Lymphotropic Virus ..... HTLV
Nucleoside Reverse Transcriptase Inhibitor ..... NRTI
Nucleotide Reverse Transcriptase Inhibitor ..... NtRTI
Phytohaemagglutinin ..... PHA
SRC Homology 3 Domain SH3
Positive Transcription Elongation Factor ..... P-TEFb

ABSTRACT

THE EFFECTS OF EXTRACELLULAR VESICLE-ASSOCIATED KINASES ON HIV-1 PATHOGENESIS

Gifty A. Mensah, Ph.D.

George Mason University, 2022

DissertationDirector: Dr. Fatah Kashanchi

As of 2020, there were 37.7 million people living with Human Immunodeficiency Virus type 1 (HIV-1). Although great strides have been made in treatment options for HIV-1 and our understanding of the HIV-1 life cycle has vastly improved since the start of this global health crisis, a functional cure remains elusive. One of the main barriers to a cure is latency, which allows the virus to persist despite combined antiretroviral therapy (cART). Recently, we have found that extracellular vesicles (EVs), membrane-bound particles released by virtually all cell types and known to mediate intercellular communication, as being responsible for the increased transcription observed in HIV-1-latently-infected cells. This study elucidates the molecular mechanism by which EVs derived from uninfected T-cells activate latent HIV-1. Our results show that kinases present in EVs such as c-Src initiate signal cascades that culminates in increased viral transcription via the PI3K/AKT/mTOR pathway. In addition, kinome profiling of EVs

revealed that the kinases CDK10, GSK3β, and MAPK8 are differentially expressed in EVs from uninfected versus HIV-1 infected cells. These kinases were shown to be biologically active and capable of phosphorylating substrates, as well as modulate changes in the cell cycle dynamics of recipient cells. Overall, data from this study implicate EV-associated kinases as key contributors to HIV-1 pathogenesis - specifically at the transcriptional and cell cycle control levels. These findings are significant because they could serve as the basis for improving and supplementing the current antiretroviral treatment regimen.

CHAPTER ONE: INTRODUCTION

Despite the great strides that have been made in the fight against HIV-1, it remains a global health crisis. As of 2020, the WHO reported that approximately 37.7 million people were living with HIV/AIDS worldwide (1). In the United States alone, an estimated 1.1 million people are infected with HIV, with over 36,000 cases diagnosed annually (2). Although a definitive cure for HIV does not exist, combination antiretroviral therapy (cART) has improved the quality of life of patients living with HIV-1 (3). cART blocks viral spread by targeting various stages of the HIV-1 replicative life cycle including entry/fusion, reverse transcription, integration and maturation, thereby forcing the infected cell into a state of latency where viral particles are below detection level (i.e., <50 copies/mL plasma) (4). However, HIV-associated neurocognitive disorders (HAND) occurs in over 47% of HIV patients despite cART (5). In addition, low level viral RNA have been found to be present in immune cells of patients under long-term cART who are considered latently infected (6, 7). This has been partially attributed to poor accessibility of antiretrovirals to sanctuary sites such as the brain and differences in cell turnover of infected cell types. In all, this calls for the need for a better understanding and improved approaches in the study of the molecular mechanisms behind latency, as well as the HIV-1 life cycle.

Latency is one of the major hurdles when it comes to completely eradicating HIV-1 as cART is unable to target latent reservoirs within various parts of the body including $CD4^+$ T-cells and macrophages, and sanctuary sites such as the testes and brain (8). Recently, the lack of transcriptional latency despite cART has been brought to the forefront. A study performed by Dornadula *et al.* revealed that viral RNA (average 17 copies/mL) was present in the peripheral blood plasma and genital tract fluids of patients under cART (9). Similarly, another study found low-level viral replication in 4 different tissue reservoirs – cerebrospinal fluid (CSF), lymphoid tissues, genitourinary tract, and serum – of patients receiving cART for 2 years (10). Furthermore, Ishizaka *et al*. reported prematurely terminated short HIV-1 transcripts (STs), which are the initial product (60 to 70 nucleotides) of viral transcription that are not affected by subsequent processes such as transcriptional elongation and alternative splicing steps, in the peripheral blood mononuclear cells (PBMCs) of both untreated and treated HIV-1 patients who have undetectable viremia in plasma (11). ST levels strongly correlated with immune activation, suggesting the possibility of using STs as biomarkers for tracking viral activation. Furthermore, another study found the presence of defective proviruses, which the authors dubbed "zombie" proviruses due to their inability to produce intact viruses but could still cause harm by generating viral nucleic acids and proteins, in patients at all stages of HIV-1 infection including before and after cART (12). The authors discovered that these defective proviruses were not silent and could potentially contribute to HIV-1 pathogenesis by producing novel unspliced HIV-1 RNA transcripts that contained a part of the *gag* and *nef* genes, as well as elements of *pol*, *env*, and *rev* (12). Taken together,

these studies clearly point to a lack of transcriptional latency despite the presence of cART. This persistent low-level viral replication in patients under cART who have undetectable plasma viremia could contribute to the failure of complete HIV-1 elimination in these individuals.

A potential mechanism contributing to the lack of transcriptional latency and residual viral replication may be the functions of extracellular vesicles (EVs), which are membrane-bound vesicles released from virtually all cell types of the body. They are present in numerous biological fluids including synovial fluid, breast milk, blood, urine, and saliva (13). EVs were originally thought to be mere vesicles utilized by cells to dispose of unwanted waste. However, it has now been established that EVs are major players in numerous essential molecular processes including inflammation, intercellular communication, cell proliferation, neuronal function, and cell survival (14). EVs contain proteins, lipids, and RNA; which can be transferred to neighboring cells, eliciting functional changes in the recipient cell (14). EVs can be categorized based on their size ranging from 30 to 5000 nm in diameter (15). For instance, exosomes typically range from 30 to 200 nm in diameter and originate from multivesicular bodies (MVBs) (15, 16). Classical exosomal marker proteins include Alix, TSG101, HSC70, HSP90β, CD63, CD9, and CD81 (15). Microvesicles (MVs) measure between 100 nm to 1 μm in diameter. Microvesicles are secreted by budding or blebbing from lipid rafts or caveolar plasma membrane microdomains (17). MVs released by cancer cells are known as oncosomes sizing up to 10 μm in diameter (15, 18). Markers of MVs include ARF6, VAMP3, and Annexin A1 (18). Apoptotic bodies are about 50 to 5000 nm in diameter

and are released by cells undergoing apoptosis. As such, apoptotic bodies have been found to contain organelles, chromatin, and small amounts of glycosylated proteins, with histones, HSP60, and GRP78 serving as protein markers (15). Recently, 2 more EV subtypes known as exomeres and supermeres have been discovered. Both exomeres and supermeres are less than 50 nm in size; and have markers such as HSP90β and Ago1, respectively (15, 19). Common isolation techniques used to separate various EV types include differential ultracentrifugation (DUC), density gradient centrifugation, size exclusion chromatography, and polymer-based precipitation (20).

EVs have been implicated in numerous pathological conditions such as cancer, cardiovascular diseases, neurological disorders, inflammatory diseases, and infectious diseases such as Ebola Virus, Rift Valley Fever, Zika Virus, and HIV-1 (21–26). It has been shown that the contents of EVs could reflect the physiological and pathological state of the parent cell (27). In the case of HIV-1, viral products such as transactivation response (TAR) RNA, a short stem-bulge-loop structure present at the 5'ends of all HIV-1 spliced and unspliced mRNAs that serves as the binding site for the viral protein Tat to enhance transcription, can be packaged into EVs and taken up by neighboring cells, resulting in the suppression of apoptosis as well as the release of pro-inflammatory cytokines (23, 28, 29). EVs have also been found to enhance HIV-1 infection by regulating the cellular transfer of co-receptors such as CCR5 and CXCR4 to receptor-deficient cells (30, 31). Consequently, EVs have been dubbed the "Trojan horses" of viral infections where viruses use them to traffic various viral products into a susceptible host cell (32).

Recently, we discovered that exosomes from uninfected cells activate transcription of latent HIV-1 (33). Data showed that upon treatment of latent HIV-1-infected cells with EVs from uninfected T-cells and monocytes, a significant increase in both TAR RNA and genomic RNA copies ensued (33). Similar results were observed in primary cells derived from 3 independent healthy donors treated with exosomes isolated prior to infection with HIV-1 dual-tropic strain 89.6. Results showed the addition of uninfected exosomes to HIV-1-infected peripheral blood mononuclear cells (PBMCs) under cART led to an increase of TAR RNA in all 3 donors while 2 out of the 3 donors saw an increase in genomic RNA levels upon exosome treatment (33). Taken together, these results suggest that exosomes from uninfected cells activate latent HIV-1. However, the mechanism of activation of latent HIV-1 was not clear. The current study aims to: 1) define the molecular mechanism underlying the EV activation of latent HIV-1; and 2) work to overcome the inability of current cART treatment in preventing HIV-1 transcription by examining the contents and effects of EVs released from HIV-1-infected cells on recipient cells (**Fig. 1**). We hypothesize that protein kinases present in EVs initiate a signal cascade that culminates in functional changes in the recipient cell including the phosphorylation of cellular substrates, alterations in cell cycle dynamics, and activation of latent HIV-1.

To elucidate the mechanism behind the EV-mediated activation of latent HIV-1, we first examined EV protein cargo. Kinases emerged as potential candidates driving the activation of latent HIV-1 due to their function as molecular switches with the ability to regulate a plethora of biological processes including cell cycle regulation, differentiation,

survival, proliferation, and immune responses. Kinases phosphorylate over 30% cellular proteins and are known for mediating signal transduction processes (34). Furthermore, kinase deregulation has been well established to play an important role in the development of numerous diseases such as cancer, cardiovascular, and infectious diseases (35, 36). Several kinases, along with their accompanying signaling pathways, have been implicated in HIV-1 pathogenesis. For instance, phosphatidylinositol 3-kinase (PI3K) plays a role in viral entry where the PI3/AKT signaling pathway is activated upon the interaction between HIV-1 envelope protein and the host CD4 receptor (37). A study done by Hamada *et al.* reported that the inhibition of the PI3K p110α by a small molecule inhibitor known as PIK-75 dampened HIV-1 entry in permissive cells and reduced the HIV-1-mediated phosphorylation of AKT (37). Similarly, the Hemopoietic Cell Kinase (Hck), expressed primarily in myeloid cells, has been shown to be activated by the viral protein Nef via the interaction of its proline-rich motif with the Hck SH3 domain (38). Interestingly, Hck was shown to be present in EVs isolated from the plasma of HIV-1 patients (39). It was found that the Nef-mediated activation of Hck prompted the activation and packaging of ADAM17, the sheddase of TNF, into plasma EVs, potentially contributing to the progression of viral infection by altering immune responses stemming from the release of TNF (39). Lastly, kinases have been implicated in the regulation of HIV-1 latency. Wolschendorf *et al*. reported that inhibition of Jun N-terminal protein kinase (JNK) using the kinase inhibitor AS601245 blocked the reactivation of HIV-1 in both cancer T-cell lines and primary T-cells despite high NF-κB activity achieved by phorbol esters or CD3/CD28 antibody costimulation (40).

Collectively, these studies demonstrate the undeniable role kinases play in HIV-1 pathogenesis.

Due to their role in a vast range of cellular processes, kinases have emerged as prime drug targets. Furthermore, the fact that the current cART regimen lacks an FDA-approved transcription inhibitor led us to explore whether EV cargo include kinases that could change the fate of recipient cells. We discovered that EVs derived from uninfected T-cells contain kinases such as c-Src, a member of the Src family of kinases (SFKs), which is involved in several signal transduction pathways that regulate cell migration, differentiation, metabolism, cell growth, cell division, immune response, and apoptosis (41). We found that c-Src initiates a signal cascade that culminates in the activation of latent HIV-1 via the PI3K/AKT/mTOR pathway (42). In addition, our kinome profiling data of EVs derived from uninfected and HIV-1-infected monocytes and T-cells revealed the presence of over 180 kinases - several of which were found to be differentially expressed between EVs and their parental cells; as well as between EVs derived from uninfected cells versus those from HIV-1-infected cells.

Moving forward, we prioritized 3 kinases based on their potential to influence HIV-1 pathogenesis. These kinases were: cyclin-dependent kinase 10 (CDK10), glycogen synthase kinase-3 beta (GSK3β), and mitogen-activated protein kinase 8 (MAPK8). CDK10 has been shown to control the function of the transcription factor, ETS2, which has in turn been found to control lymphotropic factors essential to HIV-1 transcription such as NFAT, NF-κB/p65, c-Jun, and c-Fos (43). GSK3β has been implicated in regulating Tat-mediated transcription where knockdown of GSK3β using an inhibitor

resulted in the blockage of viral replication by more than 50% after 7 and 14 days in primary cells (44). MAPK8 is part of the MAP kinase pathway which is known for transcriptional regulation of activator protein 1 (AP-1), a transcription factor integral to HIV-1 gene expression (45). Liu *et al.* reported that the viral accessory protein, viral protein R (Vpr), activates NF-κB and AP-1, leading to stimulation of the HIV-1 LTR promoter (45). Our results from this study revealed that CDK10, GSK3β, and MAPK8 present in EVs are biologically active and able to phosphorylate substrates. Lastly, these EV-associated kinases were found to change the cell cycle dynamics of recipient cells. This is important because HIV-1 replication is tied to cell cycle control. For instance, Vpr has been shown to block infected cells from proliferating by hindering the normal cell cycle control – specifically preventing cells from passing into mitosis (46). Mechanistically, Vpr was reported to cause a halt in the cell cycle at the G2 phase by interacting with the Cul4 E3 ubiquitin ligase complex, which is responsible for ubiquitinating a variety of substrates involved in cell cycle regulation (47). This further proves the intricate link between the cell cycle and HIV-1 pathogenesis. Overall, data from this current study implicate EV-associated kinases as key contributors to HIV-1 pathogenesis, specifically at the transcriptional and cell cycle control levels. These findings are significant because they could serve as the basis for improving and supplementing the current antiretroviral treatment regimen.

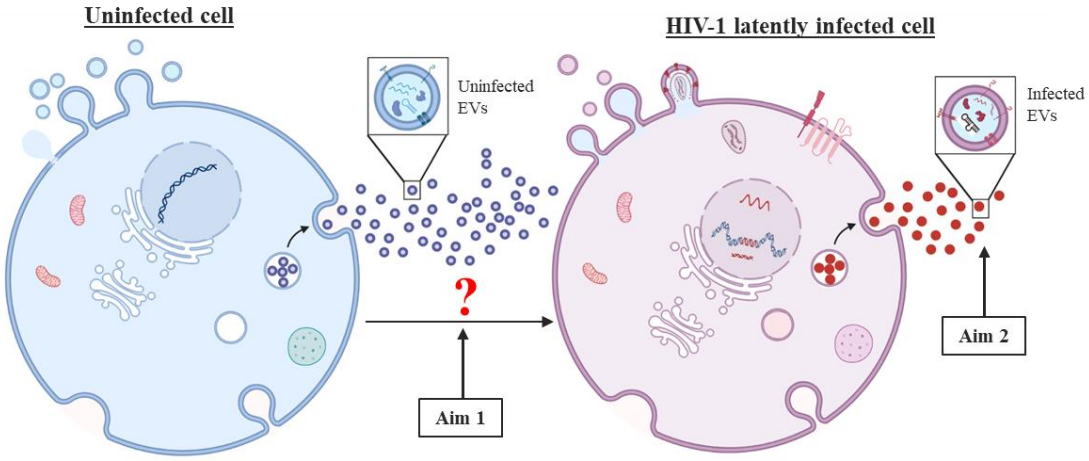

Figure 1: Summary of the specific aims for this study. This current study aims to: 1) define the molecular mechanism underlying the EV activation of latent HIV-1; and 2) examine the contents and effects of EVs released from HIV-1-infected cells on recipient cells.

CHAPTER TWO: MATERIALS AND METHODS

Cell culture and reagents

CEM (uninfected T-cell), THP-1 (uninfected monocyte), U937 (uninfected promonocytic cell), ACH2 (chronically HIV-1-infected T-cell), THP89GFP (latently HIV-1-infected monocyte), U1 (HIV-1-infected promonocytic cell), and HUT102 (HTLV-1-infected T-cell) were cultured in RPMI-1640 medium supplemented with 10% heat-inactivated exosome-depleted fetal bovine serum (FBS), 2 mM L-glutamine, 100 U/mL penicillin, and 100 µg/mL streptomycin. Exosome-depleted FBS was obtained through ultracentrifugation at 100,000 × *g* for 90 minutes to remove bovine exosomes. Dasatinib (Sellekchem, S1021), Gefitinib (Sellekchem, S1025), LY294002 (Sellekchem, S1105), MK2206 2HCl (Sellekchem, S1078), Rapamycin (Sellekchem, S1039), WP1066 (Sellekchem, S2796), Bufalin (Cayman Chemicals, 465-21-4), AZD2858 (Cayman Chemicals, 16728), NVP-2 (Cayman Chemicals, 34725), and DB07268 (Cayman Chemicals, 22257) were used to treat cells in various experiments. α-c-Src (Santa Cruz Biotechnology, sc-19), α-CD63 (Systems Bioscience, EXOAB-CD63A-1), α-Hck (Santa Cruz Biotechnology, sc-374100), α-Lck (Santa Cruz Biotechnology, sc-433), α-Fyn (Santa Cruz Biotechnology, sc-434), α-p24 (NIH AIDS Reagent Program, 4121), and α-Actin (Abcam, ab49700) were used in Western blots. α-CDK10 (Cell Signaling, 36106), α-GSK3β (Cell Signaling, 12456), α-JNK (Santa Cruz Biotechnology, sc-7345), and α-IgG (Santa Cruz Biotechnology, sc-66931) were used in Western blot, immunoprecipitation, and kinase assays.

EV isolation using Differential Ultracentrifugation (DUC)

CEM, THP-1, U937, ACH2, THP89GFP, U1, and HUT102 cells were grown in complete RPMI media with exosome-depleted FBS for 5 days. EVs were isolated from 100 mL of cell culture supernatant (10^6 cells per mL). Cell culture was spun at 500*g* for 10 minutes to get rid of cell debris. The supernatant was collected and spun at 2000*g* for 45 minutes to obtain 2K EV pellet followed by another spin at 10,000*g* for 45 minutes to yield 10K EV pellet. The resulting supernatant was then spun at 100,000*g* for 90 minutes for 100K EV pellet. Lastly, the subsequent supernatants were spun at 167,000*g* for 4hrs and 16hrs to acquire the 167K(4hr) and 167K(16hr) EV populations, respectively. Each spin was followed by a wash with PBS. All spins were performed at 4^{o}C.

EV isolation using size exclusion chromatography: IZON qEV Columns

The 35nm qEV original Gen 2 exclusion column was used according to the manufacturer's protocol. Briefly, the column was equilibrated with 1 mL PBS prior to loading of 150 μL 100K EVs suspended in PBS on top of the column. This was followed by collection of a 1 mL void volume. Next, 40 fractions of 200 μL each were collected. Fractions were pooled together in sets of 5 and concentrated with nanotrap particles (described below) followed by Western blot analysis.

Enrichment of EVs/virions using Nanotrap (NT) particles

Nanotrap particles (Ceres Nanosciences, Inc.) were used to enrich EVs from 1 mL cell-free supernatant samples as previously described (48). Briefly, a 30% slurry of NT082 (Ceres #CN2010), NT080 (Ceres #CN1030), and 1 × Phosphate Buffered Saline (PBS) or 50% slurry of NT86 (Ceres #CN1080) and 1 × PBS were combined; and 35 μL was added to 1 mL of each sample supernatant to capture EVs. The samples were then rotated overnight at 4 °C and centrifuged at 12,000 rpm for 10 minutes. The resulting pellet was washed once with PBS and used for downstream assays.

EV characterization with ZetaView Nanoparticle Tracking Analysis (NTA)

EVs isolated from cancer cell lines and PBMCs via differential ultracentrifugation were quantified and sized using the ZetaView® Z-NTA (Particle Metrix) and its corresponding software (ZetaView 8.04.02). One hundred nanometer polystyrene nanostandard particles (Applied Microspheres) were used to calibrate the ZetaView instrument prior to sample readings at a sensitivity of 75 and a minimum brightness of 20. For each reading, the instrument pre-acquisition parameters were set to a temperature of 23 °C, a sensitivity of 85, a frame rate of 30 frames per second (fps), and a shutter speed of 250 (42, 49). EVs were diluted in PBS prior to being loaded into the cell. Measurements by ZetaView were taken at 11 different positions throughout the cell, with 3 cycles of readings at each position. The mean, median, mode (indicated as diameter) sizes, and concentration were then calculated by the ZetaView software and analyzed using the same software and Microsoft Excel.

Treatment and infection of PBMCs with dual-tropic 89.6 HIV-1

Peripheral blood mononuclear cells (PBMCs) samples obtained from 3 independent donors were plated and activated with PHA/IL-2 every other day for a total of one week (29, 38). EVs were isolated from each PBMC via ultracentrifugation (100K) prior to infection with HIV-1 89.6 dual-tropic strain at an MOI of 10. Cells were then incubated for 72 hours. On Day 2 post infection, cells were treated with PHA/IL-2 followed by treatment with IL-7 and a cART cocktail a day later. The cART cocktail was repeated every other day for a week and comprised of equal parts of lamivudine (NRTI), tenofovir disoproxil fumarate (NtRTI), emtricitabine (NRTI), and indinavir (protease inhibitor) at 10 µM each. This was followed by 0.5 µM and 2.5 nM of dasatinib and bufalin, respectively, for 2 hours. The EVs isolated prior to infection of PBMCs were added back to the respective PBMCs at a ratio of 1:5000 cell per EV and allowed to incubate for 72 hours. Cells were harvested for RT-qPCR while HIV-1 virions were captured from the cell supernatant using nanoparticles (described above) for Western blot.

Cell lysis

Cells were collected and spun at 500*g* for 10 minutes. The supernatant was then discarded. The resulting pellet was washed with PBS and re-suspended in an appropriate amount of lysis buffer (50 mM Tris-HCl at pH 7.5, 120 mM NaCl, 5 mM EDTA, 0.5% NP-40, 50 mM NaF, 0.2 mM Na3VO4, and one complete protease cocktail tablet), and vortexed. Cells were incubated on ice for 20 minutes with vortexing every 5 minutes.

Cell debris was removed by centrifuging at 15,000 × g for 10 minutes at 4 °C. Total protein concentration on the resulting lysate was performed by Bradford assay (Bio-Rad) using the manufacturer's instructions.

Immunoprecipitation

Immunoprecipitation of EV-associated kinases was done by incubation of 500 μL of EVs suspended in PBS with 10 μg of kinases primary antibody (α-c-Src, α-CDK10, α-GSK3β, α-MAPK8) and 100 μL TNE50 + 0.1% NP40 overnight at 4 ^{o}C. Immunocomplexes were precipitated with a 20 μL of Protein A/G bead 30% slurry (Calbiochem) for 2 hours at 4 °C. Samples were then washed twice with TNE buffer (10 mM Tris, 100 mM NaCl, 1 mM EDTA) and used for kinase assay (described below).

Kinase Assay

EVs were lysed using lysis buffer (50 mM Tris–HCl, pH 7.5, 0.5 M NaCl, 1% NP-40, 0.1% SDS) supplemented with protease cocktail (Sigma). Immunoprecipitation (described above) was performed with the EV lysates. IPs were then washed twice with TNE buffer (10 mM Tris, 100 mM NaCl, 1 mm EDTA). Kinase assay was carried out at 37 °C for 30 minutes in a kinase assay buffer (50 mM HEPES-KOH, pH 7.9, 10 mM MgCl2, 6 mM EGTA, 2.5 mM DTT) containing 1 μg of purified histone H1 as a substrate. The reaction was halted by the addition of Laemmli buffer. Samples were separated by reducing SDS-PAGE on a 4–20% Tris–glycine gel. Gels were stained with Coomassie blue, destained, washed, and then dried for 2 hours. The dried gel was then

exposed to a PhosphorImager cassette and analyzed utilizing Molecular Dynamic's ImageQuant Software.

Western blot analysis

Whole cell extracts (WCE) or nanotrap mixture samples were resuspended in Laemmli buffer, heated at 95 °C for 3 minutes, centrifuged at 12,000 rpm for 5 minutes, loaded onto a 4–20% Tris-glycine gel (Invitrogen), and run at 200V for an hour. Proteins were transferred onto PVDF membranes (Millipore) at 50mA overnight. Gels were Coomassie-stained with 40% methanol, 7% glacial acetic acid, and Coomassie Brilliant Blue (Bio-Rad). Membranes were then blocked for 30 minutes with PBS containing 0.1% Tween 20 (PBS-T) and 5% dry milk at 4 °C. Primary antibody against specified proteins were incubated with membranes overnight at 4 °C. Membranes were washed thrice with PBS-T and incubated with appropriate HRP-conjugated secondary antibody in PBS-T for 2 hours at 4 °C. Following two washes with PBS-T and one wash with PBS, membranes were developed with Clarity Western ECL Substrate (Bio-Rad) and visualized by the Molecular Imager ChemiDoc Touch system (Bio-Rad).

RNA isolation, generation of cDNA, and Real-Time Quantitative PCR (RT-qPCR)

Total cellular RNA was isolated using Trizol reagent (Invitrogen) per the manufacturer's instructions for the quantitative analysis of HIV-1 RNA. Total RNA was used to generate cDNA using the GoScript reverse transcription system (Promega) following the manufacturer's protocol. The specific reverse primers used were: TAR Reverse (5′-CAA

CAG ACG GGC ACA CAC TAC-3′, Tm = 58 °C) (for HIV-1 TAR RNA) or Envelope Reverse (5′-TGG GAT AAG GGT CTG AAA CG-3′; Tm = 58 °C) (for HIV-1 genomic RNA). This was followed by qPCR analysis, which was done using 2 µL of undiluted aliquots of cDNA per sample with iQ Supermix (Bio-Rad) and the following primers specific for target TAR sequences: TAR Reverse (5′-CAA CAG ACG GGC ACA CAC TAC-3′, Tm = 58 °C) and TAR-Forward (5′-GGT CTC TCT GGT TAG ACC AGA TCT G-3′, Tm = 60 °C). HIV-1-infected 8E5 cell (CEM T-cell line containing a single copy of HIV-1 LAV provirus per cell) DNA serial dilutions were used as DNA standards. The PCR conditions used were: one cycle at 95 °C for 2 minutes, 41 cycles at 95 °C for 15 seconds and 58 °C for 40 seconds. DNA absolute quantification was determined based on the cycle threshold (Ct) value compared to the standard curve. All Real-time PCR reactions were carried out in triplicate using the CFX96 Real Time System (Bio-Rad).

Cell transfection

For siRNA transfection, 4 µL 100 µM siGENOME SMARTpool siRNA (Horizon Discovery) against c-Src was added to Attractine reagent at a ratio of 1.5 µL Attractine:1 µL of siRNA, mixed, and incubated for 1 hour at room temperature. siRNA against c-Src was added to ACH2 and CEM cells at a final concentration of 100 nM and incubated for 72 hours at 37 °C. ACH2 cells were then plated in 3% FBS media while siRNA-treated CEM cells were ultracentrifuged (100K) to isolate EVs. An EV titration of either 10^9 or 50^9 CEM EVs were added to the ACH2 cells. siRNA-treated CEM EVs were added to serum starved (1% FBS) U1 and ACH2 cells for another experiment at a cell to EV ratio

of $1:10^3$, $1:10^4$, or $1:10^5$. All samples were allowed to incubate at 37 °C for 48 hours. NT86 nanoparticles were added to cell supernatants and analyzed by Western blot for HIV-1 Gag p24.

Kinome profiling of EVs using peptide arrays

Kinomic profiling was performed at the University of Alabama at Birmingham (UAB) Kinome Core using the PamStation 12 platform (PamGene) as previously described (50). CEM, THP-1, and THP89GFP EVs were isolated via DUC (100K). Cells and EVs were then lysed using a lysis buffer containing 50 mM Tris-HCl at pH 7.5, 120 mM NaCl, 5 mM EDTA, 0.5% NP-40, 50 mM NaF, 0.2 mM Na3VO4, and one complete protease cocktail tablet. Ten micrograms of lysates were loaded unto arrays imprinted with tyrosine and serine/threonine phosphorylatable peptides composed of 12 to 15 amino acids. Phospho-specific fluorescein isothiocyanate (FITC)-conjugated antibodies were used to detect peptide phosphorylation. Significant differences ($p < 0.05$) in kinase activity of phosphopeptides between samples was determined using BioNavigator software, version 5 (PamGene).

EV labeling and fluorescent microscopy

To label CEM and ACH2 EVs, 20 μL of EVs were mixed with 2 μL of BODIPY 493/503 (Invitrogen) and incubated for 30 minutes at 37 °C. The mixture was then ran on a Pharmacia G-50 spin column to remove unbound dye. Labeled EVs were then characterized using ZetaView NTA (described above) prior to addition onto recipient

cells at a ratio of 1:5000 cell per EV. This was followed by imaging with an EVOS-FL-Auto microscope (Life Technologies) under 20X and 40X magnification with phase objective and fluorescence.

Cell viability assay

Fifty thousand cells in fresh RPMI media were plated in technical triplicates on a 96-well plate, followed by treatment with inhibitors. Cells were allowed to incubate for 48 hours followed by assessment for cell viability using Cell-Titer Glo reagent Luminescence Viability Kit (Promega) at a 1:1 ratio according to the manufacturer's instructions. RPMI media alone was used as background to normalize values.

Proteinase K protection assay

ACH2 EVs were isolated via DUC (100K). ACH2 EVs were treated with proteinase K at a concentration of 0.5 mg/ml proteinase K in the presence or absence of 1% Triton X-100 and incubated for 15 minutes at 37 °C. ACH2 EVs were then IPed with antibodies against CDK10 overnight. IPs were then used for a kinase assay (as described above).

Cell cycle analysis using flow cytometry

One million CEM and U937 cells were seeded in 1% FBS RPMI media for 72 hours to induce cell cycle arrest at G0. On Day 3, media was replaced prior to treatment of cells with CEM, ACH2, U937, or U1 EVs in the presence or absence of 20 μg ICAM-1 antibody (sc-8439) at a ratio of 1:5000 cell per EV. Cells were allowed to incubate for 48

hours at 37 ºC. Cells were then harvested, washed with PBS, and fixed in 70% ethanol for 30 minutes at 4 ºC. Cells were then washed twice with PBS to remove the ethanol. For fluorescence-activated cell sorting (FACS) analysis, cells were resuspended in a staining solution of propidium iodide buffer made up of PBS, 10 ug/ml RNase A, 0.1% Triton X-100, and 50 ug/ml propidium iodide. This was followed by a 15-minute incubation period at 37 ºC. The FACS data was analyzed using a BD FACSCanto™ flow cytometer (BD Biosciences).

Statistical analysis

Standard deviations were calculated for quantitative experiments using Microsoft Excel. P-values were calculated using a two-tailed student's t-test and were considered to be statistically significant when $p < 0.05$ (*), of greater significance when $p < 0.01$ (**), and of greatest significance when $p < 0.001$ (***).

CHAPTER THREE: RESULTS

Isolation and characterization of extracellular vesicles

EVs were isolated via differential ultracentrifugation (DUC). Supernatant from CEM, THP-1, U937, ACH2, THP89GFP, and U1 cells were spun at various speeds as previously described above (see Materials and Methods). **Fig. 2A** summarizes the steps used to isolate various EV populations (i.e., 2K, 10K, 100K, 167K (4hr), and 167K (16hr)). **Fig. 2B** illustrates the characterization of these EV populations using protein markers Ago1 (small exosomes), Alix (exosomes), HSP90 (exosomes), CD63 (exosomes), and CD9 (exosomes) via Western blot (15, 18, 51). Subsequent experiments for this current study utilized the 100K EV population (**Fig. 2A,** red rectangle) which excluded the 2K and 10K EV populations. The purity of the 100K EV population comprising of large exosomes from U937, CEM, U1, ACH2, THP-1, and THP89GFP cells was confirmed by Western blot, which showed the expression of exosome-specific markers Alix, Flotillin-1, CD63, and CD9 (**Fig. 2C-D)**. Additionally, the 100K EV populations from the aforementioned cell lines were subjected to NTA analysis using Zetaview to measure average size and concentration (**Fig. 2E-F**). EV sizes ranged from approximately 100 to 170 nm in size, which falls within the range of the reported size of large exosomes (15, 52).

A)

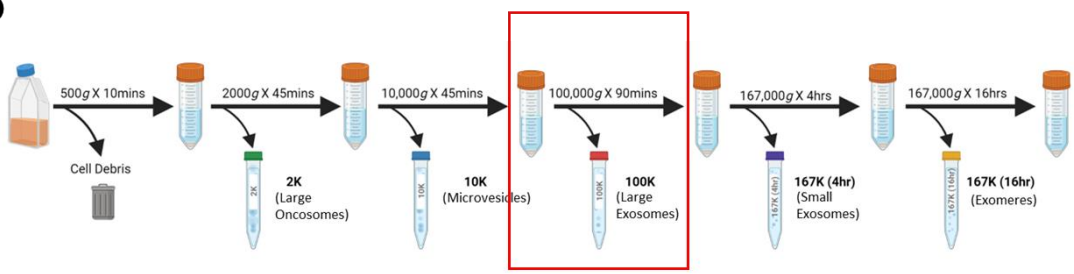
500g X 10mins
Cell Debris
2000g X 45mins
2K
(Large
Oncosomes)
10,000g X 45mins
10K
(Microvesicles)
100,000g X 90mins
100K
(Large
Exosomes)
167,000g X 4hrs
167K (4hr)
(Small
Exosomes)
167,000g X 16hrs
167K (16hr)
(Exomeres)

B)

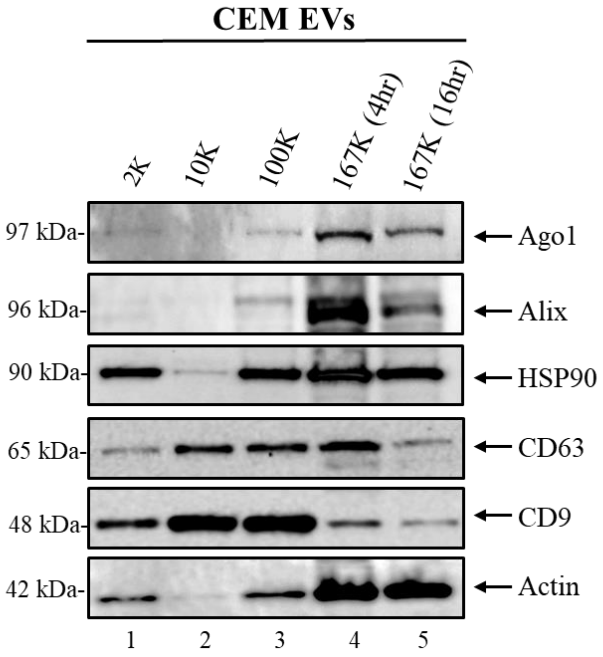
CEM EVs
2K
10K
100K
167K (4hr)
167K (16hr)
97 kDa-
96 kDa-
90 kDa-
65 kDa-
48 kDa-
42 kDa-
Ago1
Alix
HSP90
CD63
CD9
Actin
1
2
3
4
5

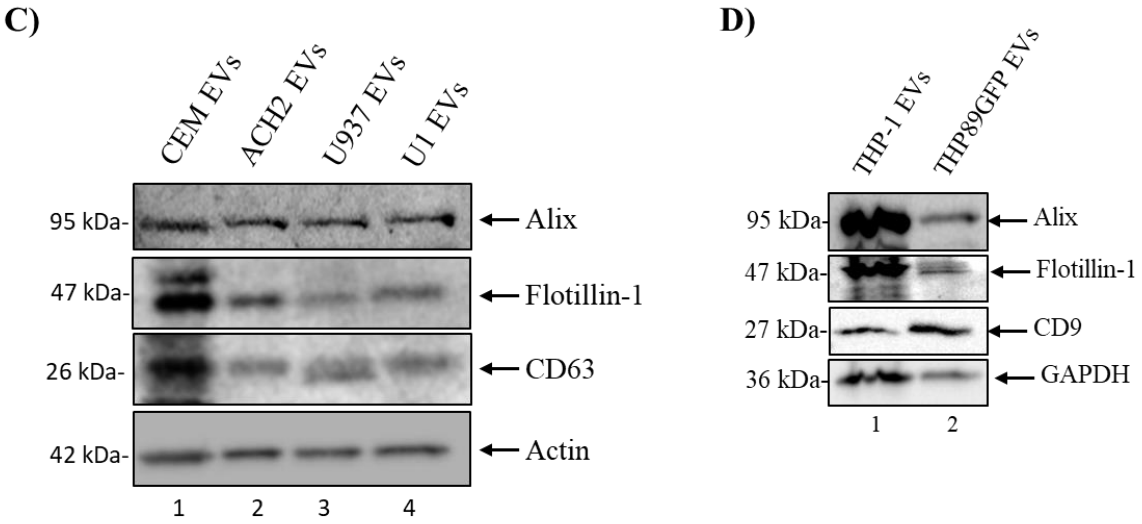
C)
CEM EVs
ACH2 EVs
U937 EVs
U1 EVs
95 kDa-
47 kDa-
26 kDa-
42 kDa-
Alix
Flotillin-1
CD63
Actin
1
2
3
4
D)
THP-1 EVs
THP89GFP EVs
95 kDa-
47 kDa-
27 kDa-
36 kDa-
Alix
Flotillin-1
CD9
GAPDH
1
2

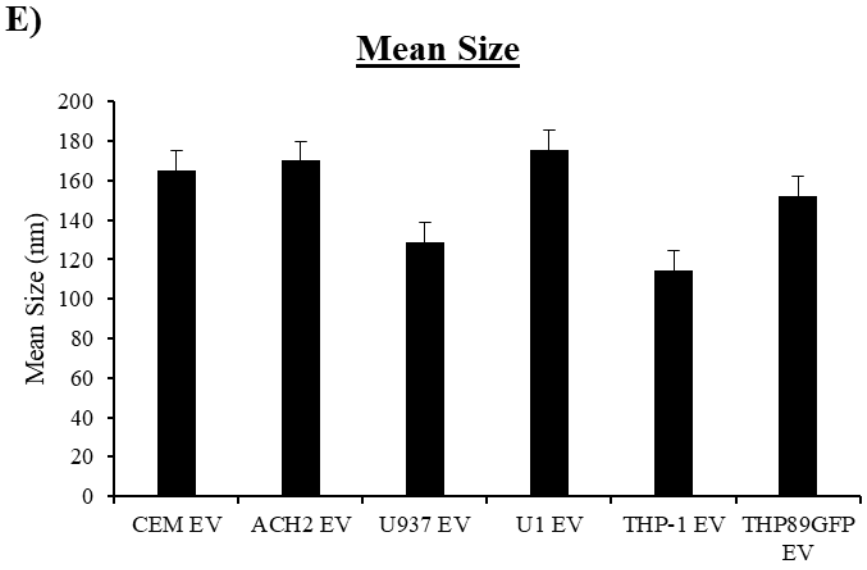
E)
Mean Size
Mean Size (nm)
200
180
160
140
120
100
80
60
40
20
0
CEM EV
ACH2 EV
U937 EV
U1 EV
THP-1 EV
THP89GFP EV

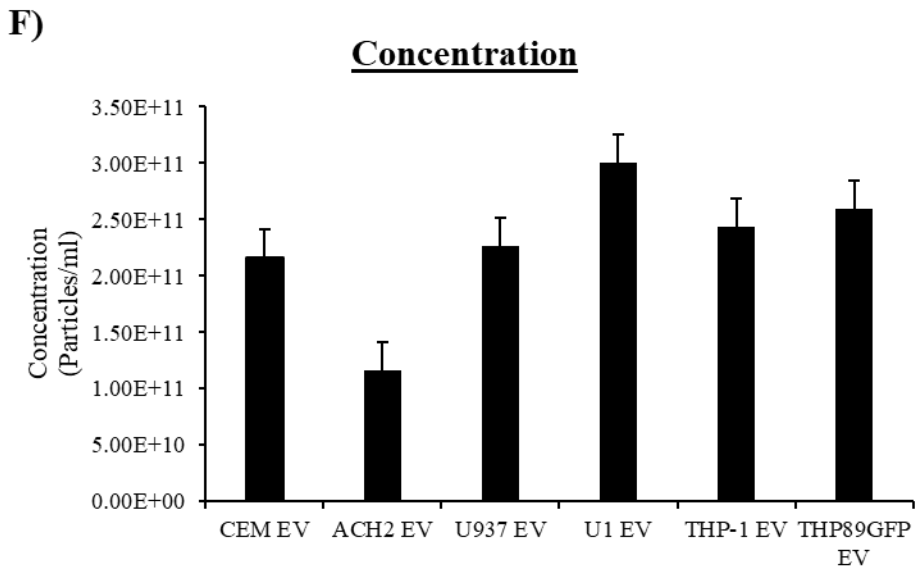

Figure 2: Characterization of EVs isolated via differential ultracentrifugation. (**A**) Schematic representation of the differential ultracentrifugation steps used to isolate various EV populations including 2K, 10K, 100K, 167K (4hr), and 167K (16hr). (**B**) CEM EV populations isolated via differential ultracentrifugation were probed for EV marker proteins Ago1, Alix, HSP90, CD63, and CD9. Actin was used as a loading control. (**C**) The 100K EV populations isolated from CEM, ACH2, U937, and U1 cells were analyzed by Western blot for Alix, Flotillin-1, CD63, and Actin. (**D**) The 100K EV populations isolated from THP-1 and THP89GFP cells were probed using Western blot to confirm the presence of Alix, Flotillin-1, CD9, and GAPDH. Size distribution analysis (**E**) and number of total vesicles released (**F**) by the 100K EV population of each cell line was estimated by ZetaView.

Extracellular vesicles contain kinases

To determine the mechanism behind the EV activation of latent HIV-1, we examined EV cargo. We focused on kinases due to their innate function of regulating several biological processes such as differentiation, proliferation, survival, migration, and immune responses; and their role in HIV-1 pathogenesis (35, 37–39, 41). Results in **Fig. 3A** demonstrate the presence of several members of the Src family kinases including Hck, Lck, c-Src, and Fyn in 10,000 EVs isolated from uninfected CEM cells. Furthermore, various EV populations (i.e., 2K, 10K, and 100K) of CEM and HUT102 (HTLV-1-infected cell line) contained c-Src (**Fig. 3B**). c-Src appeared to be enriched in the 100K

populations compared to the others in both cell lines (**Fig. 3B,** lanes 6 and 9). This observation, along with c-Src's ability to phosphorylate receptor tyrosine kinases such as EGFR to initiate signal pathways (53), prompted us to utilize the 100K EV population for subsequent experiments aimed at elucidating the signal cascade underlying the EV activation of latent HIV-1.

A)

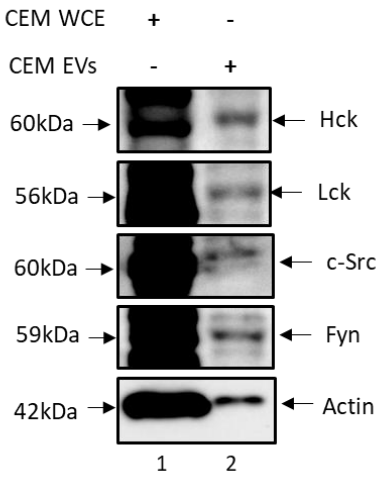

B)

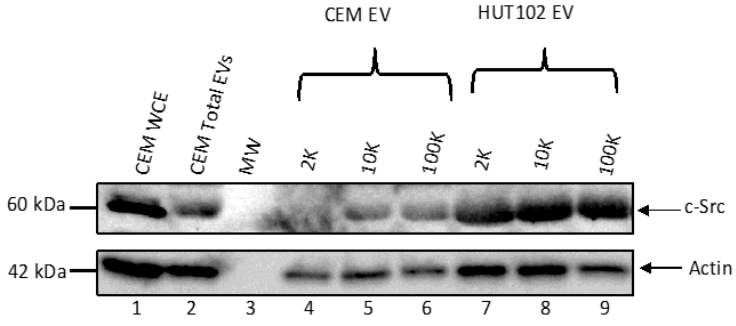

Figure 3: EVs contain kinases. (**A**) EVs (1 X 10^4) derived from CEM cells using differential ultracentrifugation (100K) were assayed for various members of the Src family of kinases including Hck, Lck, c-Src, and Fyn using Western blot. Fifty micrograms of CEM whole cells extract (WCE) served as a positive control. (**B**) EV populations 2K, 10K, and 100K were isolated from CEM and HUT102 cells via differential ultracentrifugation and probed for c-Src using Western blot. CEM WCE and CEM Total EVs (consisting of 2K, 10K, and 100K EV populations) were used as positive controls. Actin served as a loading control.

EV-associated kinases are biologically active

To test our hypothesis that EV-associated c-Src initiates a signal cascade that results in the activation of latent HIV-1 in recipient cells, we verified that EV-associated c-Src is biologically active and able to phosphorylate known cellular substrates such as Histone H1. We carried out a kinase assay using EVs derived from CEM, Jurkat, and U937 cells. EVs were enriched using NT80/82, rotated at 4^{o}C overnight, and washed with PBS prior to treatment with TNE50 + 0.1% NP40. The supernatants were then immunoprecipitated (IP) with antibodies against IgG or c-Src. The resulting complexes were then precipitated with Protein A/G beads and used for the kinase assay with histone H1 as a substrate. Data in **Fig. 4** show histone H1 was phosphorylated with c-Src from mostly T-cell EVs (lanes 4 and 8). This suggests that EV-associated c-Src is capable of phosphorylating substrates and could therefore potentially initiate a signal transduction.

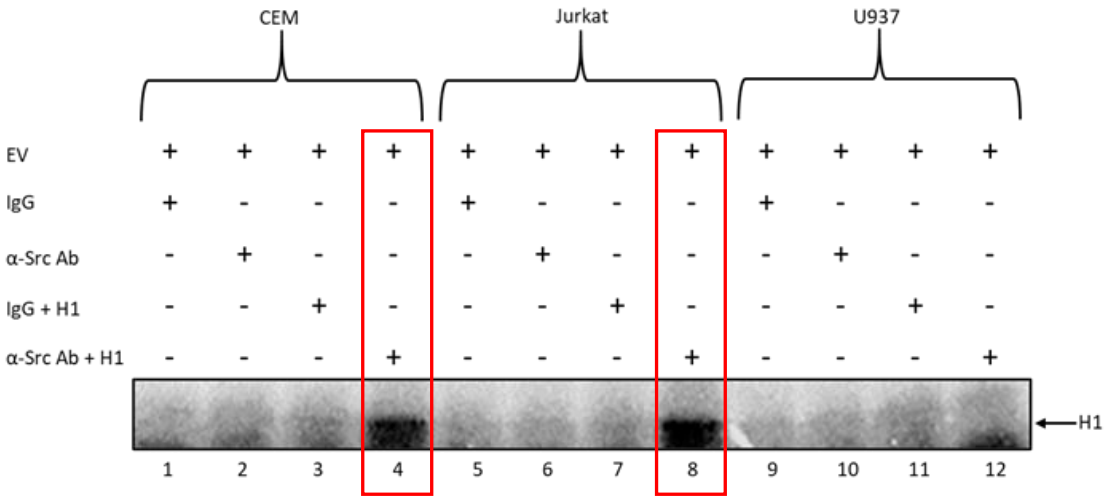

Figure 4: EV-associated kinases phosphorylate cellular substrates. (**A**) CEM, Jurkat, and U937 EVs were enriched using Nanoparticles. EVs were lysed and immunoprecipitated with IgG or α-c-Src antibody. The resulting complexes were precipitated with Protein A/G beads for 2 hours at 4ºC followed by 2 washes with TNE buffer (10 mM Tris, 100 mM NaCl, 1 mM EDTA) and kinase buffer prior to incubation with γ-32P ATP. The IPs were then used for a kinase assay with histone H1 as a substrate.

Signaling pathway of kinases linking c-Src with HIV-1 transcription

We next investigated the specific pathway employed by EVs to activate HIV-1 transcription. We began by examining known intracellular substrates of c-Src, particularly receptor tyrosine kinases (RTKs) due to their location on the cell surface. We hypothesized that c-Src activates epidermal growth factor (EGFR), an RTK which has been shown to be a downstream target of c-Src (53–55). We reasoned that this activation could lead to subsequent activation of additional kinases. EGFR has been shown to activate the PI3K/AKT/mTOR pathway, which could lead to activation of STAT3 by mTOR (56–59). The transcription factor STAT3 could then recruit SRC-1, a nuclear cofactor known for chromatin remodeling, and stimulate transcription through the recruitment of p300 and SWI/SNF (60, 61).

To test whether each of the aforementioned proteins (i.e., c-Src, EGFR, PI3K, AKT-1, mTOR, STAT3, and SRC-1) were part of the signaling pathway that leads to the activation of latent HIV-1, we employed a pharmacological perturbation approach. For this, our experimental design involved blocking the functions of each of the proteins in our proposed signaling pathway with its appropriate inhibitor as outlined in **Fig. 5A**. We treated U1 cells with inhibitors against each of the proteins. Dasatinib, gefitinib, LY294002, MK2206, rapamycin, WP1066, and bufalin were used to target c-Src, EGFR, PI3K, AKT-1, mTOR, STAT3, and SRC-1, respectively (62–66). Prior to this, we performed a cell viability assay with titrations of inhibitors to obtain the optimal concentrations needed to treat U1 cells. Data of such experiment are shown in **Fig. 5B-H**. As a result, we determined 5 µM dasatinib, 10 µM gefitinib, 10 µM LY294002, 1 µM MK2206, 150 nM rapamycin, 1 µM WP1066, and 5 nM bufalin to be the optimal dosages for subsequent experiments.

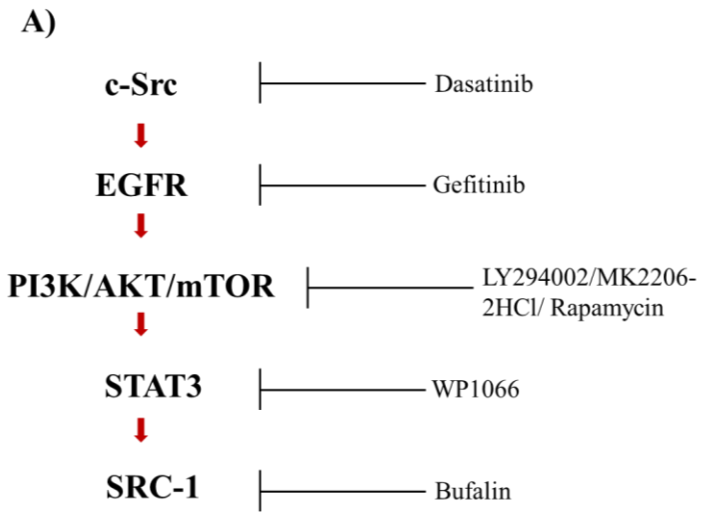

B)

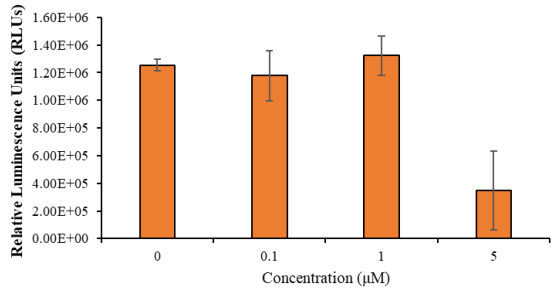
Dasatinib (U1)
Relative Luminescence Units (RLUs)
1.60E+06
1.40E+06
1.20E+06
1.00E+06
8.00E+05
6.00E+05
4.00E+05
2.00E+05
0.00E+00
0
0.1
1
5
Concentration (μM)

C)

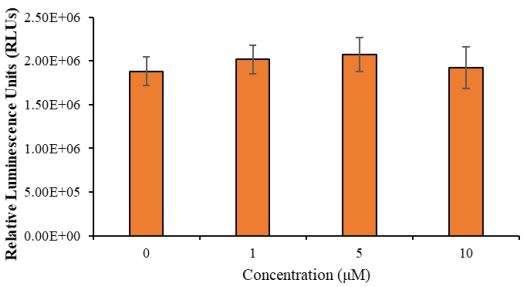
Gefitinib (U1)
Relative Luminescence Units (RLUs)
2.50E+06
2.00E+06
1.50E+06
1.00E+06
5.00E+05
0.00E+00
0
1
5
10
Concentration (μM)

D)

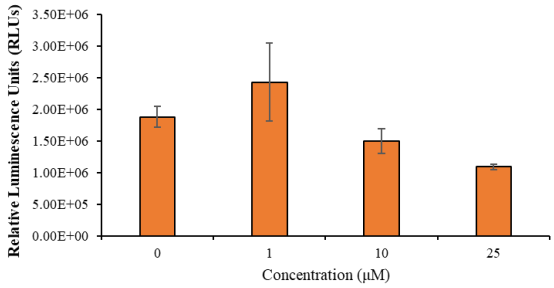
LY294002 (U1)
Relative Luminescence Units (RLUs)
3.50E+06
3.00E+06
2.50E+06
2.00E+06
1.50E+06
1.00E+06
5.00E+05
0.00E+00
0
1
10
25
Concentration (μM)

E)

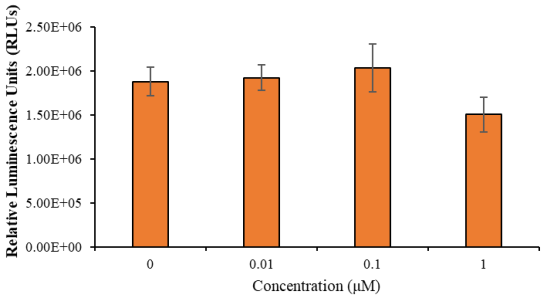
MK2206 (U1)
Relative Luminescence Units (RLUs)
2.50E+06
2.00E+06
1.50E+06
1.00E+06
5.00E+05
0.00E+00
0
0.01
0.1
1
Concentration (μM)

F)

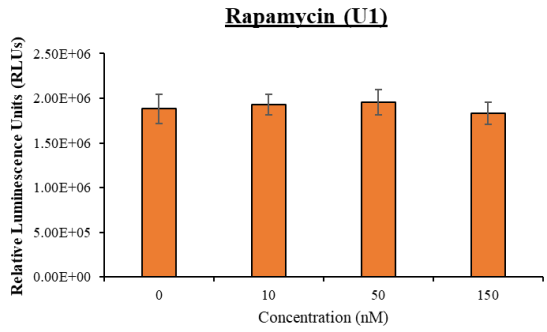
Rapamycin (U1)
Relative Luminescence Units (RLUs)
2.50E+06
2.00E+06
1.50E+06
1.00E+06
5.00E+05
0.00E+00
0
10
50
150
Concentration (nM)

G)

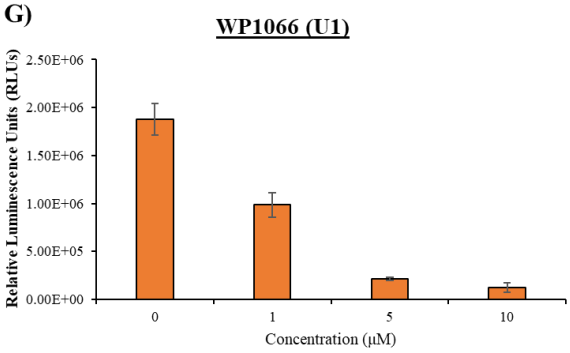
WP1066 (U1)
Relative Luminescence Units (RLUs)
2.50E+06
2.00E+06
1.50E+06
1.00E+06
5.00E+05
0.00E+00
0
1
5
10
Concentration (μM)

H)

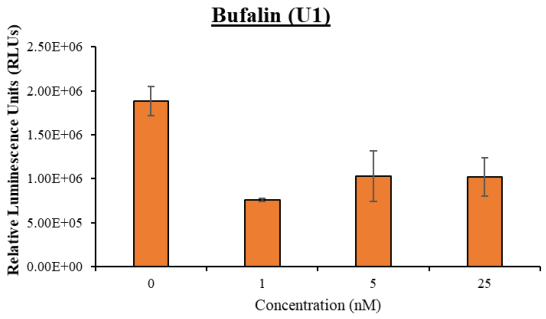

Figure 5: Inhibitor titration of HIV-1-infected monocytes. U1 cells (5×10^4) were treated with various concentrations of inhibitors and allowed to incubate for 48 hours prior to a cell viability assay. (**A**) Schematic illustration of the experimental design used to test whether specific proteins were involved in the proposed signaling pathway. U1 cells were treated with (**B**) dasatinib (c-Src inhibitor) at 0, 0.1, 1, or 5 µM. (**C**) gefitinib (EGFR inhibitor) at 0, 1, 5, or 10 µM. (**D**) LY294002 (PI3K inhibitor) at 0, 1, 10, or 25 µM. (**E**) MK2206 (AKT-1 inhibitor) at 0, 0.01, 0.1, or 1 µM. (**F**) rapamycin (mTOR inhibitor) at 0, 10, 50, or 150 nM. (**G**) WP1066 (STAT3 inhibitor) at 0, 1, 5, or 10 µM. (**H**) bufalin (SRC-1 inhibitor) at 0, 1, 5, or 25 nM. Error bars represent ± S.D. of three technical replicates for all panels. A two-tailed Student's t-test was used to assess significance: *$p < 0.05$; **$p < 0.01$; ***$p < 0.001$.

EVs containing c-Src rescue HIV-1 levels in inhibitor-treated cells

One of the goals of this study is to determine the molecular pathway underlying the EV-associated kinase-mediated activation of latent HIV-1. Therefore, we tested whether each of the proteins (i.e., c-Src, EGFR, PI3K, AKT-1, mTOR, STAT3, and SRC-1) are involved in the signaling cascade leading to the activation of HIV-1 by blocking each of the proteins with its appropriate inhibitor prior to addition of EVs containing c-Src. Briefly, U1 cells were plated and treated with various inhibitors and allowed to incubate for 48 hours. A second drug treatment was then performed. After a 2-hour incubation period, CEM EVs were added to the cells at a ratio of 1:5000 (cell:EV). Cells were then allowed to incubate for 24 hours before a second CEM EV treatment of 1:5000 (cell:EV).

Cells were then allowed to incubate for 24 hours and harvested for downstream assays. Cell pellets were prepped for RNA isolation and subsequent RT-qPCR analysis to measure the levels of HIV-1 TAR RNA and genomic RNA while cell supernatants were collected and treated with Nanotraps (NT86) overnight prior to assaying for HIV-1 Gag p24 by Western blot. Data in **Fig. 6A-B** demonstrate that treatment with inhibitors dasatinib (c-Src), gefitinib (EGFR), LY294002 (PI3K), MK2206 (AKT-1), rapamycin (mTOR), WP1066 (STAT3), and bufalin (SRC-1) decreased the levels of HIV-1 TAR RNA and genomic RNA in infected cells in comparison to the untreated control. However, upon addition of CEM EVs, cells treated with dasatinib, rapamycin, and bufalin saw increased HIV-1 TAR RNA and genomic RNA levels compared to the non-EV-treated samples highlighted by the red boxes in **Fig. 6A-B**.These results suggest that despite drugs exerting their inhibitory functions against key upstream proteins implicated in HIV-1 transcription, the addition of CEM EVs (containing c-Src) was able to override the effects of inhibitors and rescue HIV-1 TAR RNA and genomic RNA levels. Rapamycin (inhibitor against mTOR) caused the largest decease in HIV-1 TAR RNA levels (**Fig. 6A**), while treatment with bufalin (inhibitor against SRC-1) resulted in the largest decrease in genomic RNA levels (**Fig. 6B**). This implies that SRC-1 may be more important in the transcription of full-length, coding HIV-1 RNA as opposed to mTOR, which might be more vital in the transcription of shorter, noncoding HIV-1 RNA.

Lastly, to validate our RT-qPCR data, we tested for the presence of HIV-1 virions in the cell supernatant of the above experiment using Western blot. Data in **Fig. 6C-D** show increased levels of Gag p24 in all EV-treated cells despite treatment with inhibitors

compared to the non-EV-treated opposites. This was confirmed with densitometry analysis in **Fig. 6E** which outlines the dramatic increase in p24 expression upon treatment with CEM EVs. Taken together, these results suggest that EV-associated c-Src may play an essential role in the EV-mediated activation of latent HIV-1.

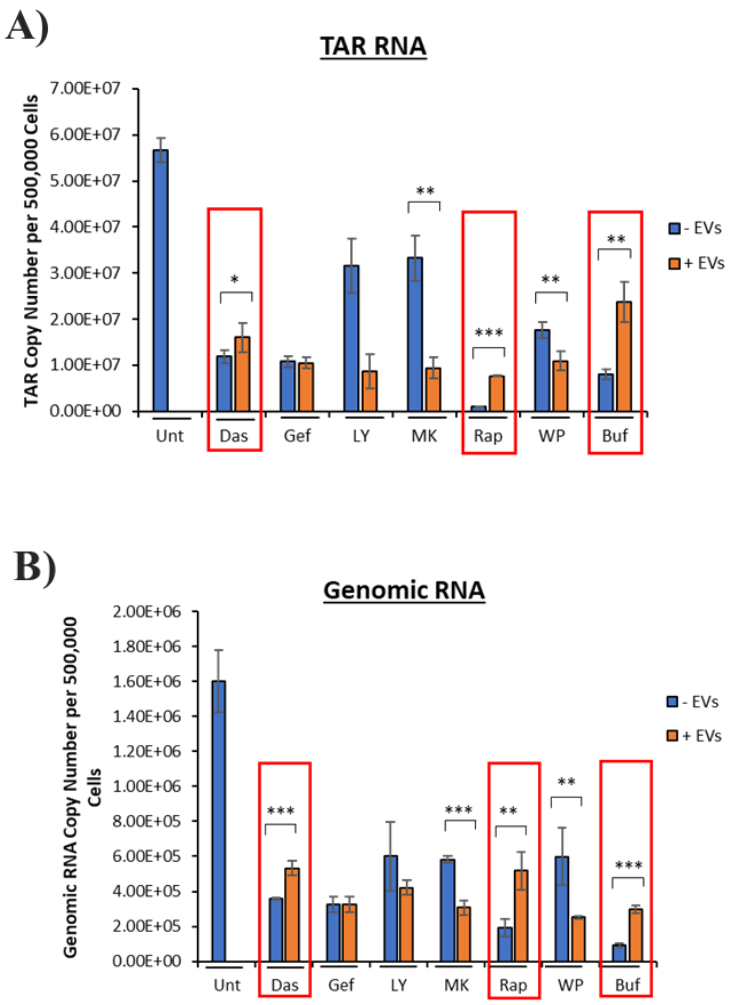

C)

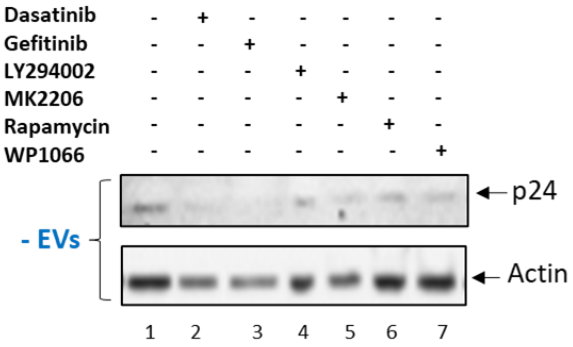
Dasatinib - + - - - - -
Gefitinib - - + - - - -
LY294002 - - - + - - -
MK2206 - - - - + - -
Rapamycin - - - - - + -
WP1066 - - - - - - +
- EVs
p24
Actin
1 2 3 4 5 6 7

D)

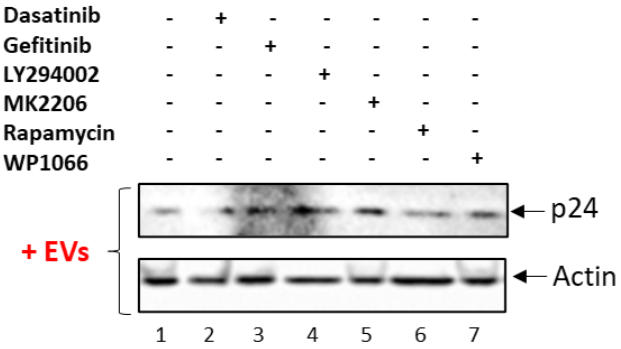
Dasatinib - + - - - - -
Gefitinib - - + - - - -
LY294002 - - - + - - -
MK2206 - - - - + - -
Rapamycin - - - - - + -
WP1066 - - - - - - +
+ EVs
p24
Actin
1 2 3 4 5 6 7

E)

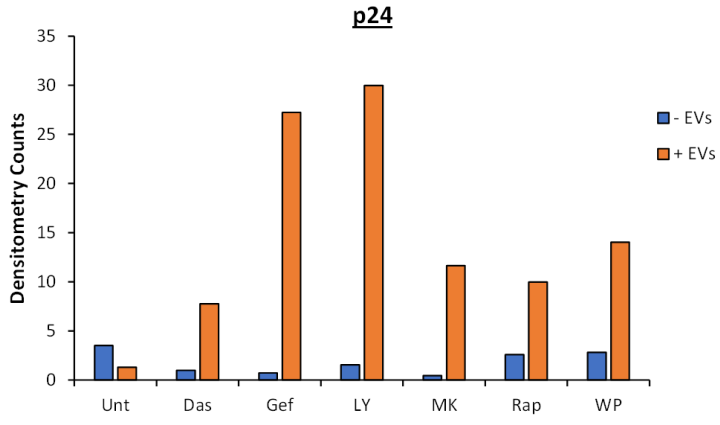
p24
Densitometry Counts
35
30
25
20
15
10
5
0
Unt
Das
Gef
LY
MK
Rap
WP
- EVs
+ EVs

Figure 6: EVs containing c-Src rescue HIV-1 RNA levels in inhibitor-treated cells. CEM EVs were isolated by 100,000 x *g* ultracentrifugation. Five hundred thousand U1 cells were plated and treated with 5 μM dasatinib, 10 μM gefitinib, 10 μM LY294002, 1 μM MK2206, 150 nM rapamycin, 1 μM WP1066, or 5 nM bufalin and allowed to incubate for 48 hours. This was followed by a second drug treatment, after which cells were allowed to incubate for 2 hours prior to the addition of CEM EVs. After a 24-hour incubation period, a second EV treatment was done. The total ratio of cells to EVs was 1:10,000. Cells were then allowed to incubate for 24 hours. Cell supernatant was collected and rotated overnight at 4 °C with NT86. Total RNA was isolated and subjected to RT-qPCR for HIV-1 TAR RNA (**A**) and genomic RNA (**B**). Red boxes indicate increased HIV-1 TAR and genomic RNA levels in EV-treated cells in the presence of dasatinib, rapamycin, and bufalin. (**C, D**) NT86-treated samples were analyzed by Western blot for HIV-1 Gag p24. U1 WCE was used as a positive control. Actin was used as a loading control. (**E**) Densitometry counts normalized to actin are shown for HIV-1 Gag p24. For all figures, EV untreated samples were used as negative controls. Student's t-test compared untreated cells with cells treated with drugs. *, $p < 0.05$; **, $p < 0.01$; ***, $p < 0.001$. Error bars, S.D.

EV-associated c-Src activates HIV-1 in latently infected cells

The Src family of protein tyrosine kinases, which include c-Src, Frk, Lck, Lyn, Blk, Hck, Fyn, Yrk, Fgr, and Yes, are key regulators of signal transductions (67, 68). In addition to c-Src, we found that Hck, Lck, and Fyn are present in CEM EVs (**Fig. 2A**). Also, other studies have shown the presence of additional src kinases such as Lck and Fyn to be present in T-cells (69, 70). Thus, we attempted to verify that c-Src, rather than other Src family member kinases, was involved in initiating the signal cascade that results in the reactivation of latent HIV-1. In the following experiment, we used CEM EVs isolated from CEM cells transfected with siRNA against c-Src to treat both U1 (HIV-1-infected monocytes) and ACH2 (HIV-1-infected T-cells) cells and assessed HIV-1 activation by measuring p24 expression using Western blot. We found that p24 expression was higher in both U1 and ACH2 cells when c-Src was present in EVs (**Fig. 7A,** lanes 2 and 7) in comparison to the controls or when c-Src was knocked down in EVs in lanes 3–5 and lanes 8–10 of **Fig. 7A**. These results suggest that c-Src may be behind the activation of HIV-1 in these infected cells.

Next, we further needed to confirm that the observed activation of HIV-1 was due to EV-associated c-Src and not intracellular c-Src. The rationale here was that intracellular c-Src, which is present in virtually all cell types (71) could be responsible for the activation of HIV-1. As such, we serum-starved ACH2 cells to force them into transcriptional silence and knocked down intracellular c-Src using siRNA against four different sequences within the c-Src gene. CEM EVs (containing c-Src) were then added to ACH2 cells and allowed to incubate for 24 hours. Western blot results in **Fig. 7B** show a dose-dependent increase in Gag Pr55 expression in ACH2 cells that were treated with CEM EVs compared to the control. Similarly, siRNA knockdown of intracellular c-Src led to minimal Gag p24 expression in ACH2 cells. This was reversed upon the addition of EVs, which resulted in a dramatic increase in p24 expression (**Fig. 7C**). Together, these data point to EV-associated c-Src as a key contributor to the activation of HIV-1.

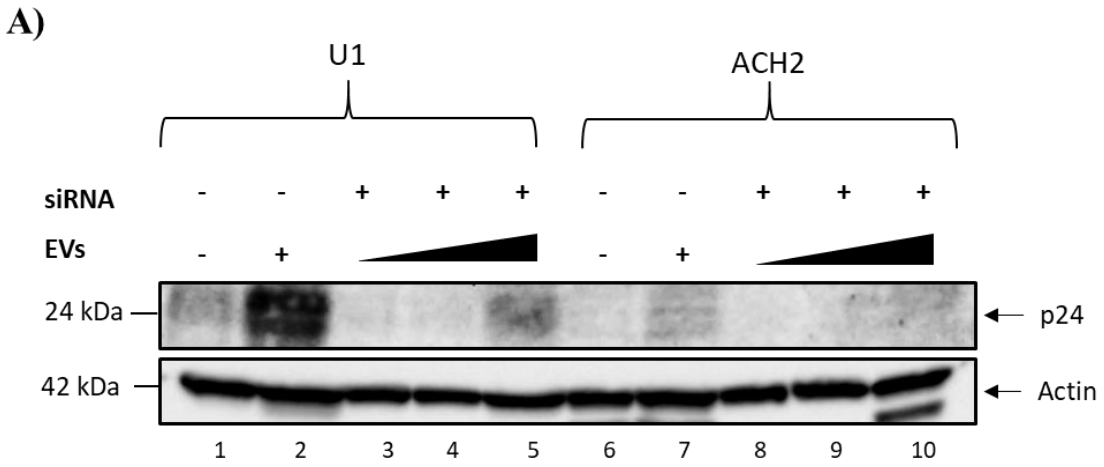

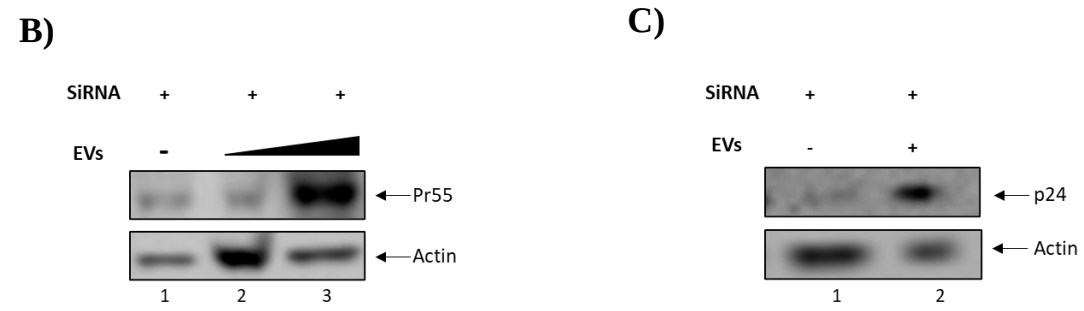

Figure 7: EV-associated c-Src activates HIV-1 in latently infected cells. (**A**) EVs were isolated via ultracentrifugation (100K) from CEM cells transfected with siRNA against c-Src. EVs were then added to serum-starved U1 and ACH2 cells at a ratio of $1:10^3$, $1:10^4$, or $1:10^5$; followed by a 24-hour incubation period and Western blot analysis for p24. (**B, C**) Serum-starved ACH2 cells were transfected with siRNA against c-Src. Cells were then treated with CEM EVs at a ratio of 0, 10^9, or 50^9 cells to EVs (**B**) or 0 or 50^9 EVs (**C**) and allowed to incubate for 72 hours followed by Western blot analysis for HIV-1 Gag Pr55 (**B**), Gag p24 (**C**). Actin was used as a loading control.

Verification of c-Src and SRC-1 roles in latent HIV-1 activation in primary cells

Next, we validated the role of EV-associated c-Src in the activation of latent HIV-1 using primary cells. Here, we obtained PBMCs from 3 independent donors and cultured them in PHA/IL-2 for 7 days. EVs were then isolated from the PBMCs via ultracentrifugation (100K) prior to infection with HIV-1 89.6 dual tropic strain. To induce latency and suppress viral spread, PBMCs were treated with cART and IL-7 every other day for 7 days. The PBMCs were then treated with 0.5 µM dasatinib and 2.5 nM of bufalin. Next, EVs (isolated prior to infection) were added back to their respective PBMC at a ratio of 1:5000 cell per EV. Cells were then harvested, and RNA was isolated and reverse transcribed for RT-qPCR (**Fig. 8A**). Results in **Fig. 8B** shows a significant increase in HIV-1 TAR expression in the presence of EVs compared to the controls. Similar results were observed in **Fig. 8C** where genomic RNA levels rose significantly upon the addition

of EVs to PBMCs. These results support earlier experiments performed in cancer lines. Collectively, these data confirm that c-Src and SRC-1 may be part of the signal pathway that activates latent HIV-1.

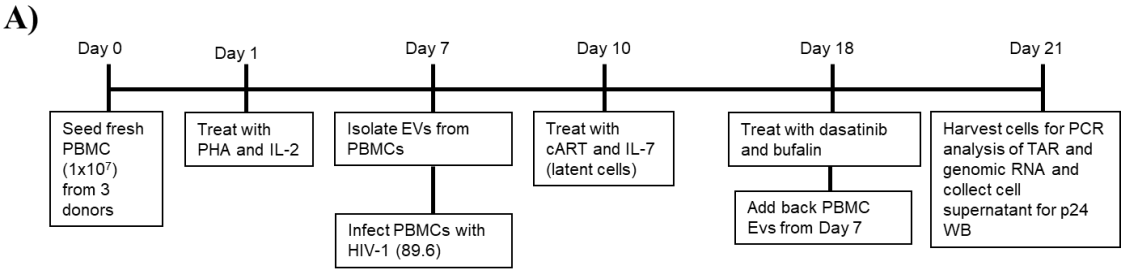

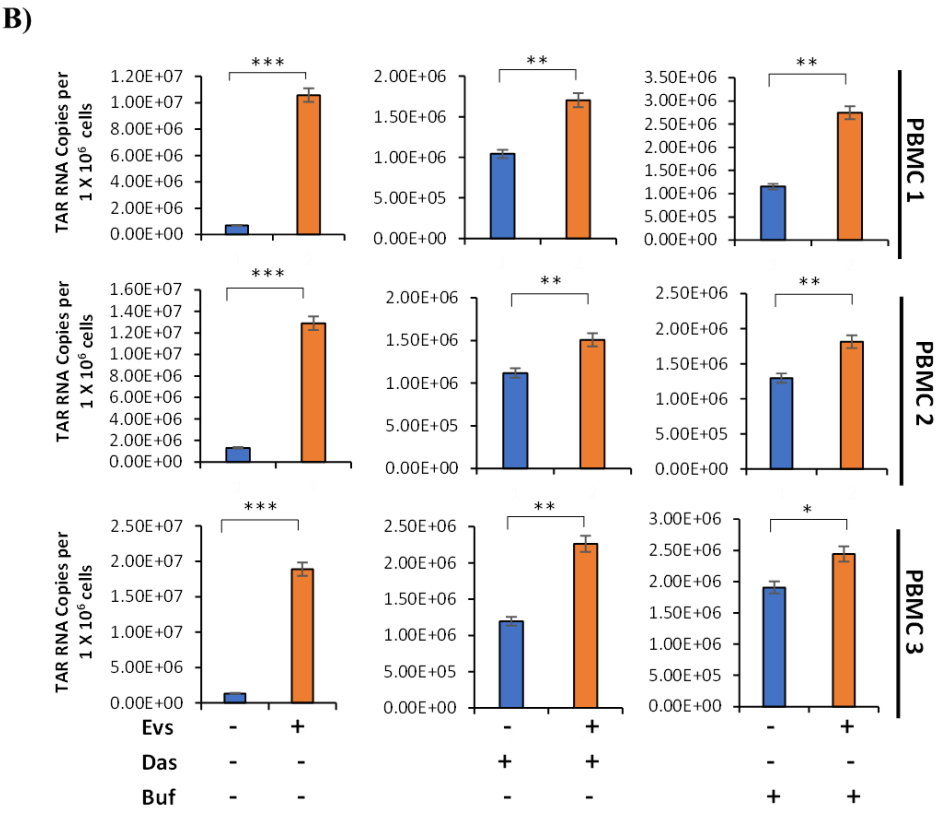

C)

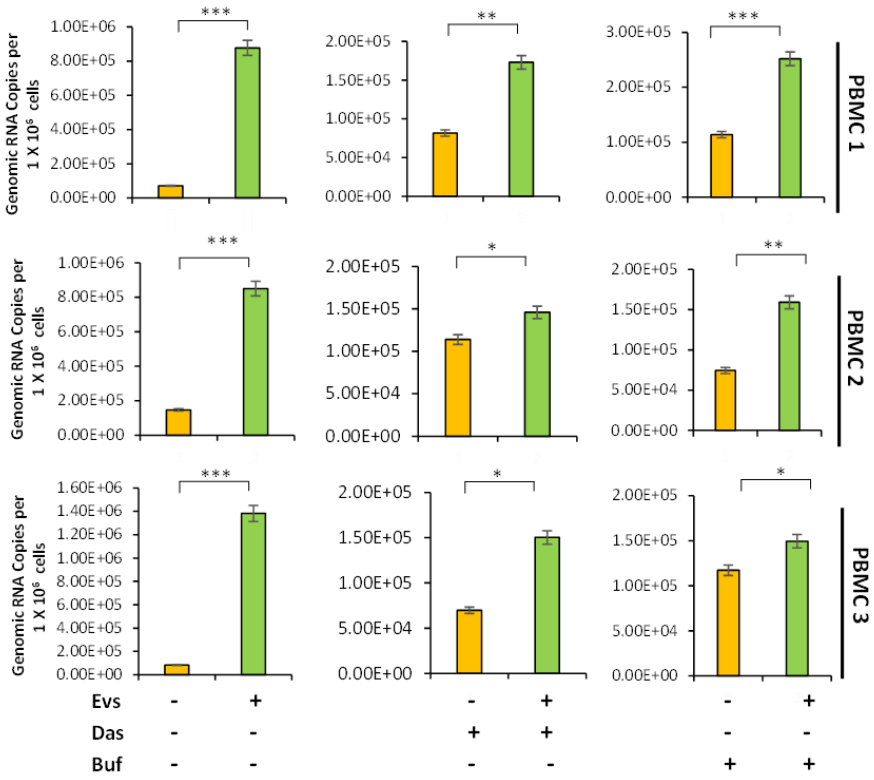

Figure 8: c-Src and SRC-1 contribute to the activation of latent HIV-1 in primary cells. (**A**)Workflow of treatment and infection of Peripheral blood mononuclear cells (PBMCs). PBMCs from 3 independent donors were treated with 2.5 nM and 0.5 µM of bufalin and dasatinib, respectively. After a 2-hour incubation period, EVs were isolated using ultracentrifugation (100K) from each of the PBMCs prior to infection with HIV-1 (89.6). EVs were then added back to each of their respective PBMCs at a ratio of 1:5000 cells per EVs. After 72 hours, cells were harvested for downstream assays. Total RNA was isolated from cell pellets and subjected to RT-qPCR for HIV-1 TAR RNA (**B**) and genomic RNA (**C**).

Proposed signaling cascade for the EV-mediated activation of latent HIV-1

In this study, we have shown that EVs derived from uninfected T-cells contain the kinase c-Src, which is able to phosphorylate substrates. Inhibition of c-Src, EGFR, PI3K, AKT-1, mTOR, STAT3, and/or SRC-1 led to decreased levels of HIV-1 TAR and genomic

RNA inside the cell as well as decreased HIV-1 Gag p24 in the cell supernatant, thereby proving the contribution of these proteins in HIV-1 activation. We propose that upon the internalization of EVs from uninfected T-cells (containing c-Src) by latently infected cells, c-Src initiates a signal cascade involving EGFR, the PI3K/AKT-1/mTOR pathway, STAT3, and SRC-1. The translocation of SRC-1 to the nucleus could lead to the recruitment of p300 to the HIV-1 promoter thereby influencing chromatin remodeling and increased loading of RNA Pol II onto the HIV-1 promoter, culminating in increased viral transcription (**Fig. 9**).

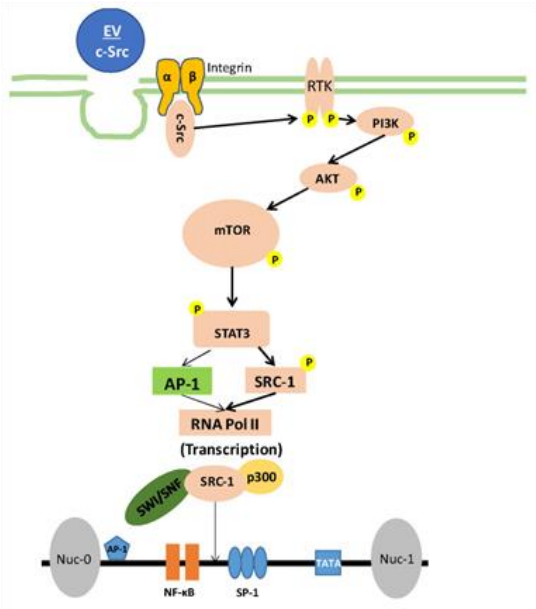

Figure 9: Proposed model for the EV-mediated activation of latent HIV-1. EVs containing c-Src from healthy cells are internalized by HIV-1-latently-infected cells, leading to the phosphorylation and activation of receptor tyrosine kinases (RTK) such as EGFR by c-Src. RTK then activates PI3K, which in turn activates AKT. AKT then phosphorylates mTOR, resulting in the phosphorylation and activation of the transcription inducer, STAT3. STAT3 recruits the cofactor SRC-1, prior to translocating to the nucleus and promoting HIV-1 transcription by recruiting p300 (promotes chromatin remodeling). NF-κB and RNA Pol II increase loading onto the HIV-1 promoter, resulting in the transcription of latent HIV-1.

Kinome profiling using peptide arrays

The second aim of this study is to examine the contents and effects of EVs released from HIV-1-infected cells on recipient cells. The rationale stemmed from a previous work where we found increased expression of CDK9 and CDK2 in EVs derived from HIV-1-infected T-cells compared to their uninfected counterparts (72). However, only a few kinases were studied and their effects on recipient cells were not explored. Here, we utilized kinome profiling to identify additional kinases present in EVs. An advantage of this method is that in addition to the identification of kinases, it also revealed changes in the phosphorylation status of several EV-associated kinases simultaneously. Briefly, EVs were isolated from CEM, THP-1, and THP89GFP cells using ultracentrifugation (100K). Cells and EVs were then lysed and loaded onto arrays imprinted with tyrosine and serine/threonine phosphorylatable peptides. Kinase activity in lysates were detected using fluorescence-conjugated antibodies (**Fig. 10**). Output analysis revealed over 180 kinases present in our EV preps.

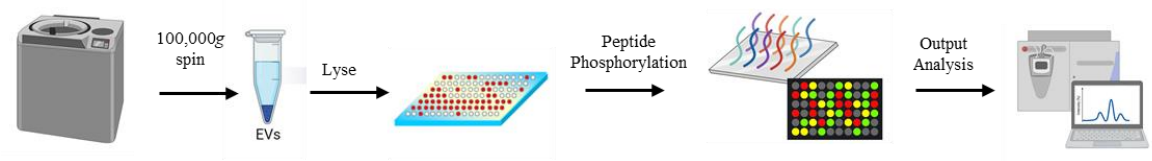

Figure 10: Workflow of EV kinome profiling. EVs were isolated from CEM, THP-1, and THP89GFP cells via ultracentrifugation (100K). EVs were then lysed and loaded onto arrays enriched with tyrosine and serine/threonine phosphorylatable peptides at a concentration of 10 μg to measure kinase activity. Fluorescence-conjugated antibodies were used to detect peptide phosphorylation.

Selection of EV-associated kinases

Next, we attempted to select and prioritize a few of the kinases out of the 180 for further analysis. The approach utilized to select specific kinases for additional testing is outlined in **Fig. 11A**. To do this, we performed statistical analysis to determine peptides with the largest increase in phosphorylation activity in the EVs derived from HIV-1-infected cells relative to the uninfected control or parental cell line; constructed heatmaps from results obtained from our kinome profiling experiment; and examined the differential expression of various kinases proteins found in EVs derived from uninfected and HIV-1-infected cell lines. Heatmaps such as the one shown in **Fig. 11B-C** revealed several kinases such as CDKL3, CDK10, PTK2, CAMK1, and MAPK8 to be upregulated in EVs derived from THP89GFP and CEM cells. To further narrow down our list of kinases to examine, we focused on those that have been documented to be associated with HIV-1 pathogenesis.

Three kinases, namely CDK10, GSK3β, and MAPK8, fit all our selection criteria and emerged as worthwhile candidates for further exploration as to their ability to influence HIV-1 pathogenesis. CDK10 has been shown to regulate the transcription factor ETS2, which mediates several genes vital to HIV-1 transcription (43). GSK3β, an integral part of signaling pathways in neurons and significantly dysregulated in several neurological disorders such as Alzheimer's disease, has been shown to mediate Tat-induced neurotoxic effects (73, 74). Inhibition of GSK3β in primary cells resulted in decreased viral transcription, suggesting its participation in regulating viral transcription (44). Similarly MAPK8 has been implicated in HIV-1 pathogenesis due to its place in the MAP kinase pathway which stimulates the HIV-1 LTR via phosphorylation of

components of AP-1 including c-Fos and c-Jun (75). **Table 1** summarizes the comparison of the relative changes in the expression levels of our 3 priority kinases. Together, these findings prompted further examination of the role EV-associated CDK10, GSK3β, and MAPK8 may play in HIV-1 replication.

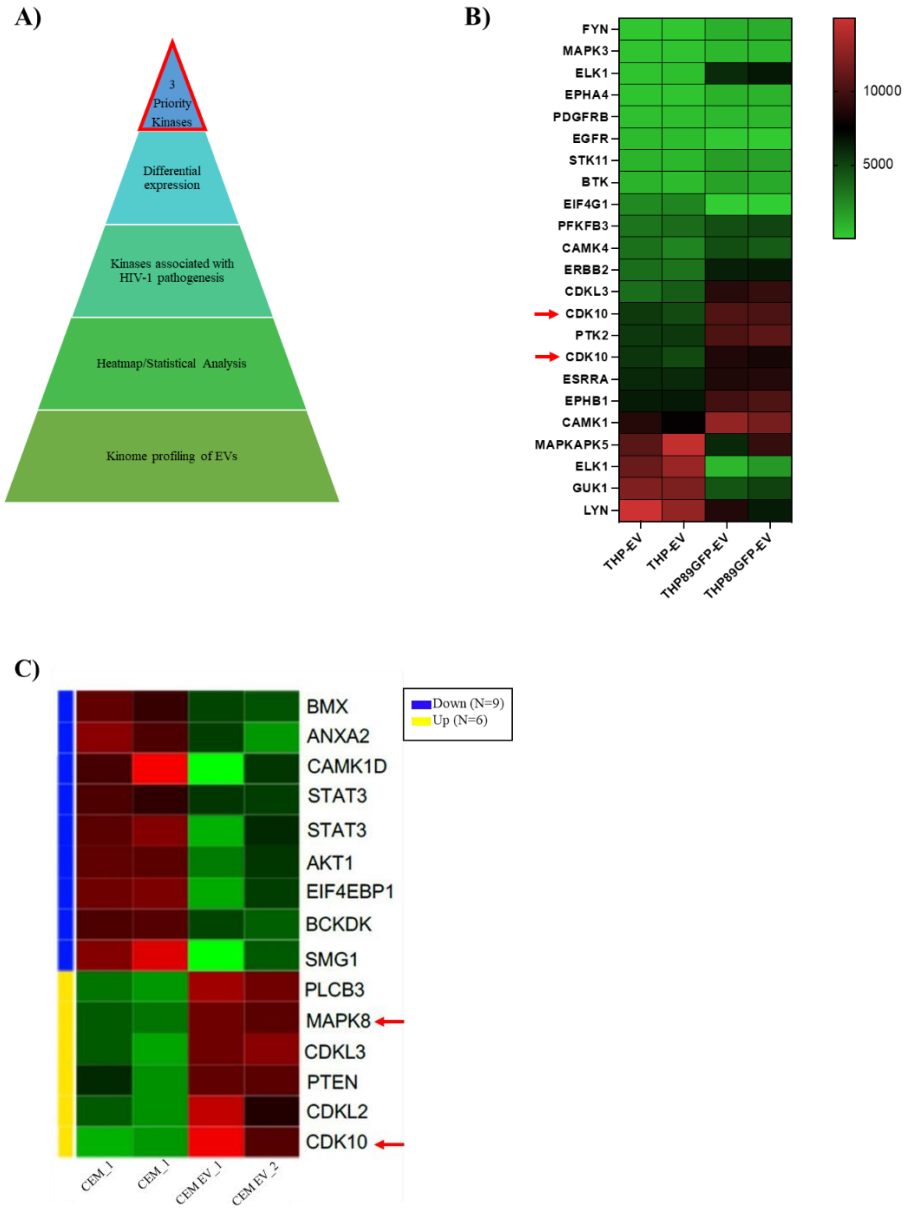

Figure 11: Selection of EV-associated kinases. (**A**) Three EV-associated kinases were prioritized for further analysis based on statistical significance, association with HIV-1 pathogenesis, and differential expression. (**B**) Heatmap showing the differential expression of peptides from EVs isolated from uninfected monocytes (THP-1) and HIV-1-infected monocytes (THP89GFP). (**C**) Representative heatmap illustrating differential expression of various peptides in CEM cells versus CEM EVs.

Table 1: Differential expression of kinases in uninfected and HIV-1-infected EVs. A summary table showing the comparison of the relative changes in the expression levels of the 3 priority kinases (CDK10, GSK3β, and MAPK8) of uninfected and HIV-1-infected EVs.

Kinase	Extracellular Vesicle	Average Normalized Net Signal	% CFC (Change from Control)
CDK10	THP-1	5092	-
	THP89 GFP	10293	102%
GSK3β	THP-1	7227	-
	THP89 GFP	9317	13%
MAPK8	THP-1	380	-
	THP89 GFP	449	18%

Kinases are differentially expressed in EVs derived from uninfected versus HIV-1-infected cells

We next sought to validate our peptide array studies using biochemical assays such as Western blot, with an emphasis on the differential expression of the 3 priority kinases (i.e., CDK10, GSK3β). This was important because differential expression between uninfected and infected EVs could signify the stimulation of certain pathways in the target cell that could potentially alter the fate of the cell. We therefore asked whether the

3 kinases are differentially expressed in EVs isolated from uninfected T-cells (CEM) and myeloids (U937) in comparison to their HIV-1-infected counterparts (ACH2 and U1, respectively). Western blot analysis in **Fig. 12A** shows MAPK8 and GSK3β are upregulated in ACH2 EVs although CDK10 was undetectable (lanes 2 and 4). Similar results were observed in the myeloids where all 3 kinases exhibited increased gene expression in the U1 EVs compared to the U937 EVs (lanes 6 and 8). To confirm the purity of our EV preps and verify that our kinases of interests are indeed associated with EVs, we performed an additional EV isolation method – size exclusion chromatography – using IZON qEV columns. Here, EVs derived from ACH2 and U1 cells via DUC (100K) were loaded onto an IZON qEVoriginal/35 nm Gen 2 columns. Forty fractions were collected and pooled in sets of 5 (1 mL final volume) followed by NT80/82 nanotrap particle treatment overnight to enrich EVs. The pooled fractions were then probed for CDK10, GSK3β, MAPK8, HSP90, and CD63 using Western blot. Results of such experiment are shown in **Fig. 12B-C** where CDK10, GSK3β, and MAPK8 (p46 and p54 isoforms) are mostly enriched in Fractions 1 through 5 followed by Fractions 6 through 10, and 11 through 15, respectively. As evidenced by the expression of the EV markers, HSP90 and CD63, in Fractions 1 through 5 (**Fig. 12B-C**, lane 4), our 3 kinases of interest (i.e., CDK10, GSK3β, and MAPK8) are enriched in the EV fractions and not the later fractions, which are associated with free proteins. Collectively, this data supports our previous findings of the presence of CDK10, GSK3β, and MAPK8 in EVs; and confirms that these 3 kinases are upregulated in EVs derived from HIV-1-infected cells.

A)

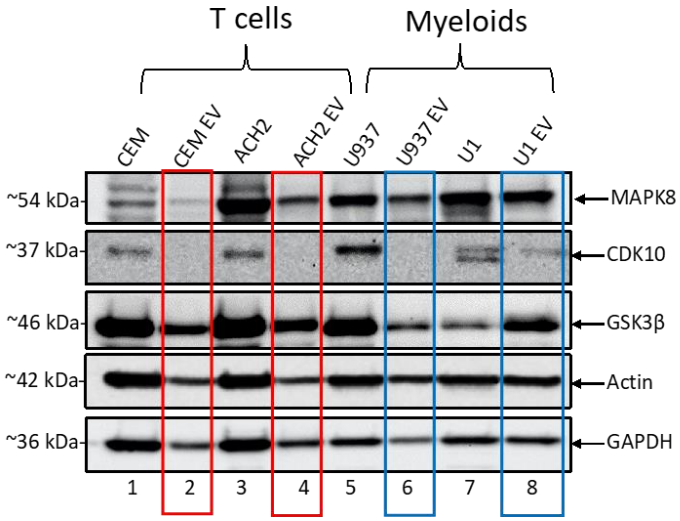
T cells
Myeloids
CEM
CEM EV
ACH2
ACH2 EV
U937
U937 EV
U1
U1 EV
~54 kDa
~37 kDa
~46 kDa
~42 kDa
~36 kDa
MAPK8
CDK10
GSK3β
Actin
GAPDH
1
2
3
4
5
6
7
8

B)

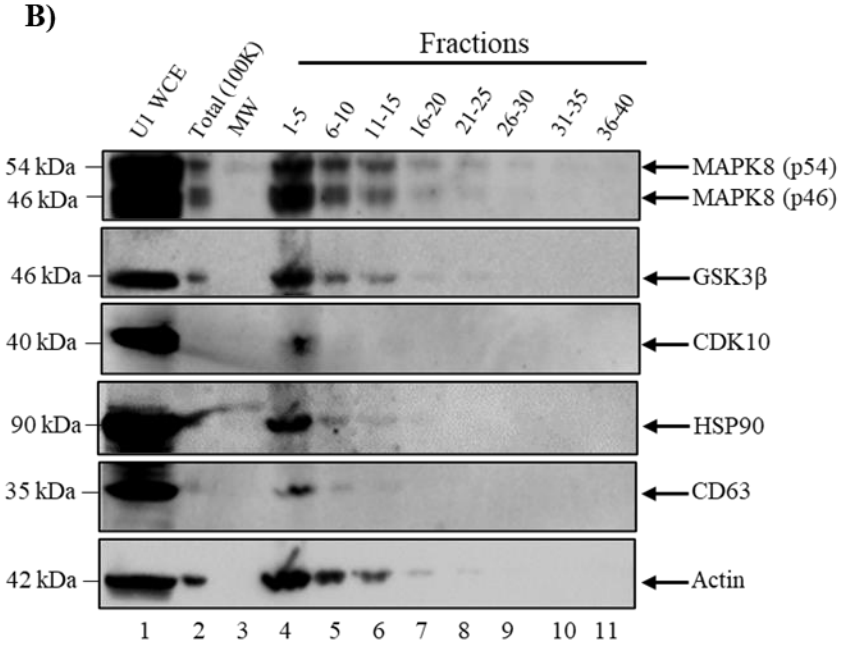
Fractions
U1 WCE
Total (100K)
MW
1-5
6-10
11-15
16-20
21-25
26-30
31-35
36-40
54 kDa
46 kDa
MAPK8 (p54)
MAPK8 (p46)
46 kDa
GSK3β
40 kDa
CDK10
90 kDa
HSP90
35 kDa
CD63
42 kDa
Actin
1
2
3
4
5
6
7
8
9
10
11

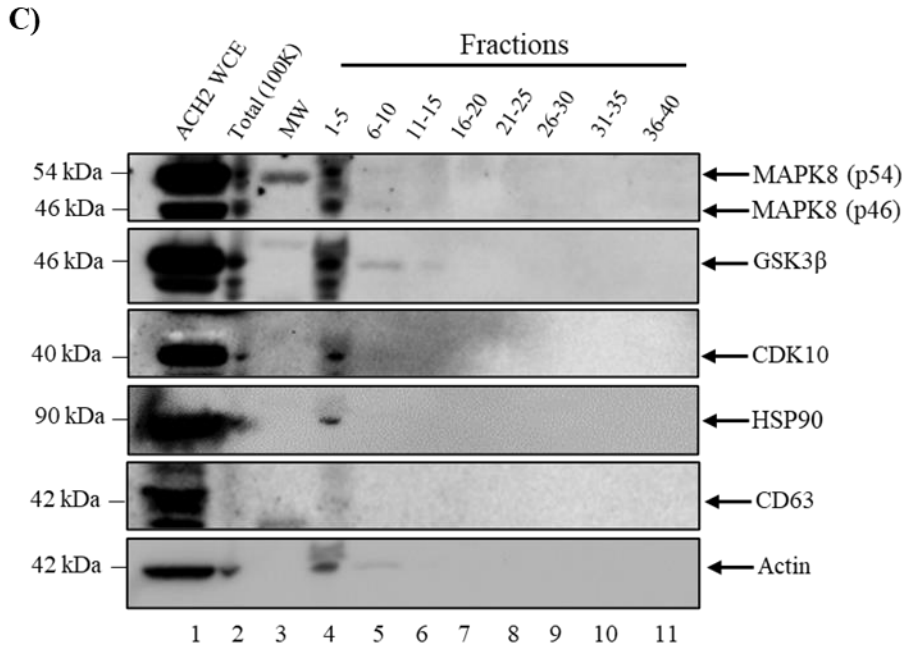

Figure 12: CDK10, GSK3β, and MAPK8 are differentially expressed in uninfected versus HIV-1-infected EVs. (**A**) EVs were isolated via differential ultracentrifugation (100K) from uninfected T-cells (CEM) and myeloids (U937); and HIV-1-infected T-cells (ACH2) and myeloids (U1). EVs were probed for MAPK8, CDK10, and GSK3β using Western blot. Actin served as a loading control. U1 EVs (**B**) and ACH2 EVs (**C**) isolated via differential ultracentrifugation (100K) were loaded onto IZON 35nm qEVoriginal Gen 2 exclusion columns. Forty fractions were collected and pooled in sets of 5. Pooled fractions were then probed for MAPK8, CDK10, GSK3β, HSP90, and CD63 using Western blot.

EVs from HIV-1-infected cells are taken up at a faster rate

Having established the differential expression of the 3 kinases of interest in uninfected and infected EVs, we suspected there may be other differences that could impact the effects of EVs on recipient cells. We therefore asked whether a difference also existed in the uptake kinetics between the two. The rationale was that if the EVs are to exert any type of functional change in recipient cells, they most likely would have to first be internalized or fuse with recipient cell membranes, which could be directly with the plasma membrane (direct uptake) or endosomal membrane (endocytic uptake). EVs are

taken up by cells through several pathways including endocytic pathways such as clathrin-dependent endocytosis, and clathrin-independent pathways such as caveolin-mediated uptake, macropinocytosis, phagocytosis, and lipid raft–mediated internalization (76). Proteins found on the surface of EVs and target cells may also influence the EV uptake mechanism (77).

Here, we visualized EV uptake with the use of a fluorescent lipophilic dye known as BODIPY. EVs isolated from CEM and ACH2 cells via DUC (100K) were labeled with BODIPY. These labeled EVs were then added onto CEM recipient cells at a ratio of 1:5000. This was then followed by fluorescence microscopy imaging at 12-, 24-, and 48-hour timepoints. Results in **Fig. 13** show that approximately 46% of CEM EVs were taken up by recipient cells in comparison to 52% for ACH2 EVs. After 24 hours of incubation, CEM cells had taken up about 53% of EVs compared to 71% of the ACH2 EVs. A similar trend was observed at the 48-hour timepoint where about 64% of CEM EVs had made it into recipient cells while 89% of ACH2 EVs had been internalized at that point. Collectively, these data suggest that EVs derived from HIV-1-infected cells may be taken up at a faster rate and higher amounts in comparison to EVs from uninfected cells.

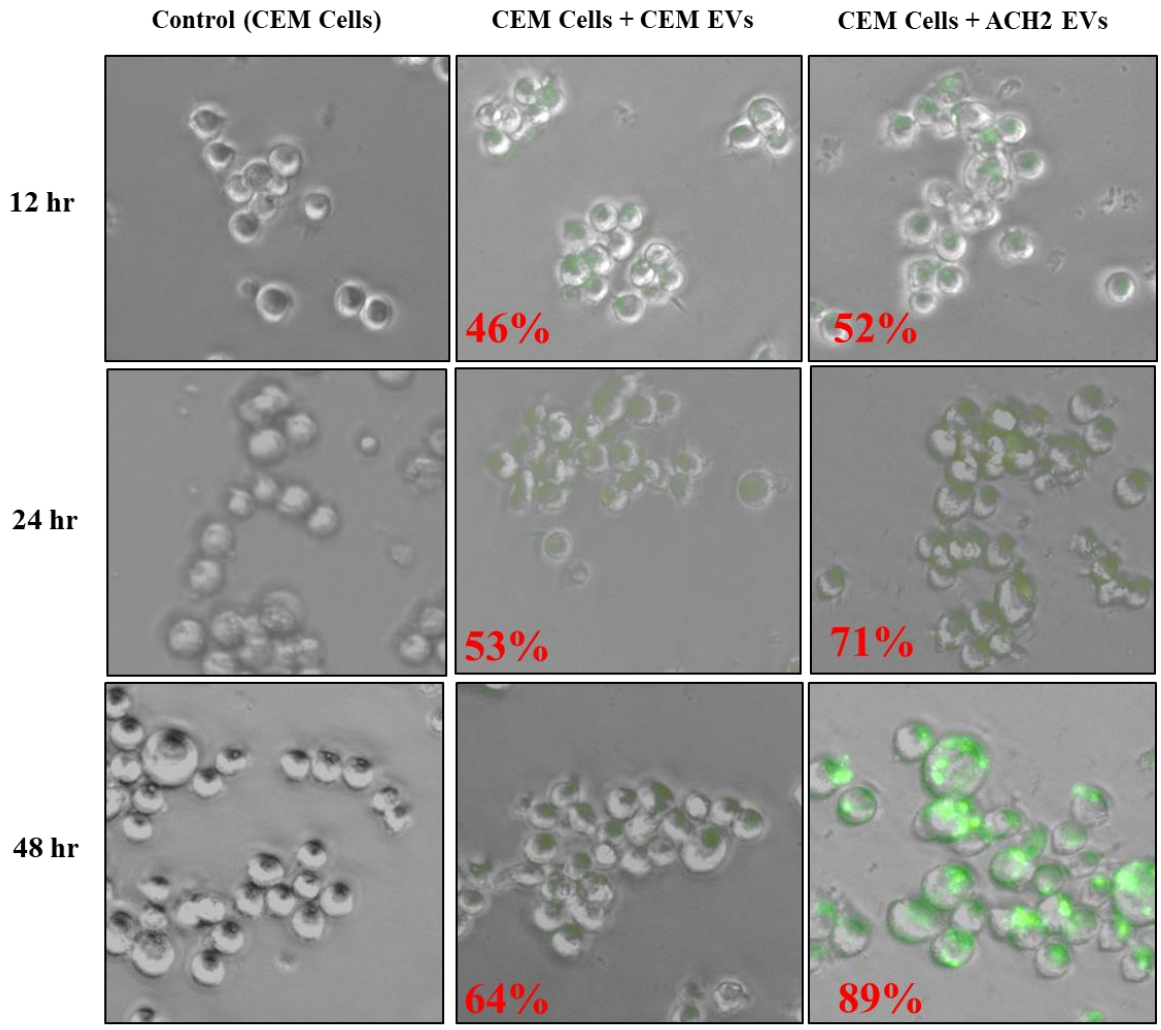

Figure 13: EVs from HIV-1-infected cells are taken up at a faster rate. EVs isolated from CEM and ACH2 cells via differential ultracentrifugation (100K) were labeled with BODIPY™ 493/503 and then incubated with CEM cells at a ratio of 1:5000 cell to EV. Fluorescence microscopy imaging was done to track BODIPY labeled EVs at 12, 24, and 48 hours.

Functional characterization of EV kinases using kinase assay

Next, we sought out to confirm whether EV-associated CDK10, GSK3β, and MAPK8 are functionally active and could phosphorylate substrates. We therefore tested their activity

on purified Histone H1 as a substrate using a radioactivity-based kinase assay. Briefly, EVs from CEM, ACH2, U937, and U1 cells were lysed and immunoprecipitated with antibodies against CDK10, GSK3β, MAPK8, and IgG (control). Complexes were then precipitated with A/G beads, washed, and incubated with radiolabeled ATP and purified histone H1. Samples were resolved by SDS-PAGE. Gels were then destained and exposed to a PhosphorImager.

As shown in **Fig. 14**, the phosphorylation of histone H1 by EV-associated CDK10, GSK3β, and MAPK8 was detectable in both T-cells and myeloid EVs. We observed that phosphorylation of histone H1 increased with ACH2 EVs (**Fig. 14A**, lanes 6-8) in comparison to the uninfected CEM EVs (**Fig. 14A**, lanes 2-4) where no significant signal was detected. Similarly, phosphorylation activity of CDK10, GSK3β, and MAPK8 from U1 EVs were higher than that of U937 EVs (**Fig. 14B**). Furthermore, densitometry analysis confirmed the dramatic increase in the phosphorylation activity of kinases derived from HIV-1-infected cells compared to uninfected cells in both T-cells and myeloids. This suggests that CDK10, GSK3β, and MAPK8 may be differentially expressed in HIV-1-infected EVs versus uninfected EVs, which would support our kinome profiling data outlined in **Fig. 11** and **Table 1**. Collectively, these data indicate that the EV-associated kinases, CDK10, GSK3β, and MAPK8, from HIV-1 infected EVs are biologically activate and capable of phosphorylating substrates, which could lead to the activation of signal transduction pathways.

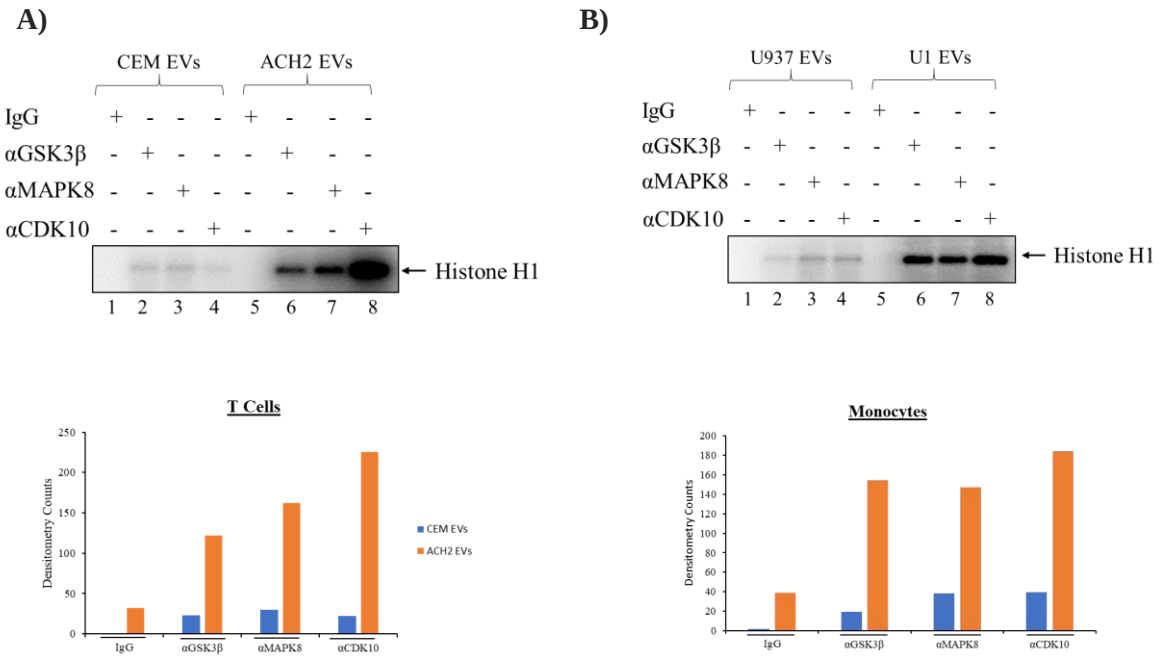

Figure 14: Functional characterization of EV-associated kinases. EVs were isolated from (**A**) CEM, ACH2, and (**B**) U937 and U1 cells via differential ultracentrifugation (100K). EVs were then lysed and immunoprecipitated (IP) with antibodies against CDK10, GSK3β, and MAPK8. IgG served as a control. IPs were then used for a kinase assay with purified histone H1 as a substrate. Densitometry analysis of the histone H1 bands was performed using ImageJ analysis software.

CDK10 is present inside EVs derived from HIV-1-infected T-cells

It has been established that EVs carry all sorts of cargo including lipids, nucleic acids, and proteins (78–81). Some of these proteins such as TSG101 and Flotillin-1 are localized in the lumen of EVs while proteins such as ICAM-1, CD63, and eCIRP are enriched on the surface of EVs (82–84). The significance of the orientation of EV protein cargo lies in the accessibility of endogenous proteases where the degradation of EV proteins would depend on their location. Consequently, if proteins are found on the surface of EVs, they would be more accessible to proteases and subsequent enzymatic

degradation during the journey through the extracellular environment compared to those found on the inside of EVs.

To determine the localization of EV-associated CDK10, we performed a protease protection assay followed by a kinase assay (**Fig. 15A**). Briefly, EVs isolated from ACH2 cells via DUC (100K) were treated with or without Triton X-100 or proteinase K and allowed to incubate for 15 minutes at 37 °C. EVs were then IPed with antibodies against CDK10 overnight. Complexes were then subjected to a kinase assay with histone H1 as a substrate. Results in (**Fig. 15B**) demonstrate that when the lipid membrane of EVs are permeabilized due to the presence of Triton X-100, proteinase K is able to get inside and digest CDK10. As such, there is no phosphorylation activity (**Fig. 15B,** lane 2). On the other hand, when Triton X-100 is absent and the EVs are intact, there is no kinase digestion and we therefore observe phosphorylation of histone H1 in lane 3 of **Fig. 15B**. Purified CDK5 kinase was used as a positive control to verify the protease activity of proteinase K on our preps. Taken together, this data suggests that CDK10 is enriched on the inside of ACH2 EVs.

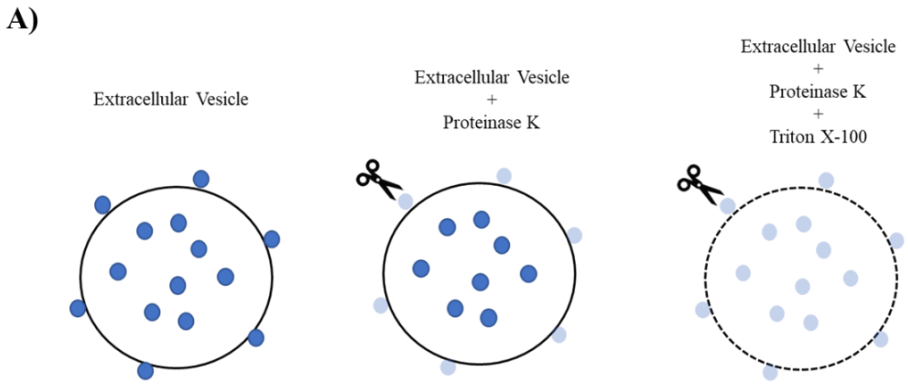

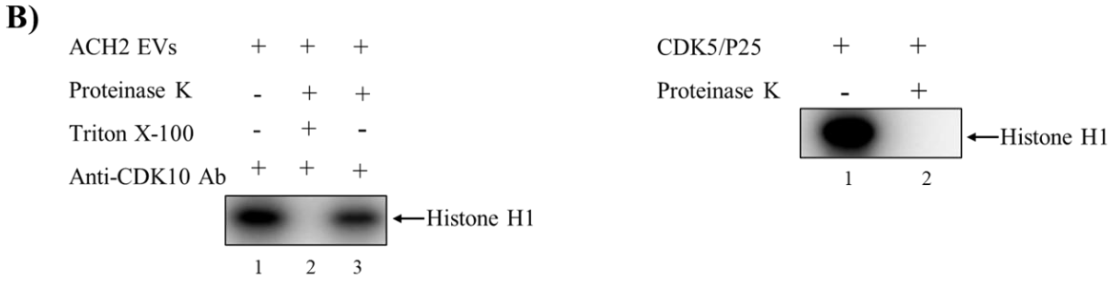

Figure 15: CDK10 is present inside ACH2 EVs. (**A**) ACH2 EVs were treated with or without Triton X-100 in the presence of proteinase K. Schematic illustration of proteinase protection assay. Adapted from (83). (**B**) EVs were then immunoprecipitated with antibody against CDK10 and used in a kinase assay. Purified CDK5 kinase was used as a positive control.

EVs modulate changes in the cell cycle dynamics of recipient cells

We next examined functional changes exerted by EVs derived from HIV-1-infected cells on recipient cells, particularly pertaining to the cell cycle. A number of studies have reported links between cell cycle regulation and viral pathogenesis. For instance, Salamango *et al*. reported that HIV-1 Vif perturbs the cell cycle by inhibiting cell cycle progression at the G2 phase via degradation of cellular protein phosphatase 2A (PP2A) regulators, which control most of the phosphatase activity in eukaryotic cells (85, 86). Similarly, another study described the role of Vif in forcing cell cycle arrest at G2 by interfering with the activation of CDK1 and cyclin B1, causing significant $CD4^+$ T-cell death (87). Lastly, Vpr has also been implicated in G2 arrest by associating with Cul4 E3 ubiquitin ligase complex (47). Thus, we asked whether EVs from HIV-1-infected cells could cause cell cycle deregulation in recipient cells.

For this, we serum starved CEM and U937 cells for 3 days followed by treatment with CEM, ACH2, U937 or U1 EVs at a ratio of 1:5000 cell per EV and incubated for 2 days. Cells treated with antibody against ICAM-1 were used as a control where ICAM-1 (found on the surface of EVs) served as an EV uptake inhibitor due to its role in exosome internalization via its interaction with LFA-1 expressed on the surface of T-cells (88). Cells were then fixed with propidium iodide prior to cell cycle analysis using flow cytometry. Cell cycle progression analysis in **Fig. 16** show that addition of EVs to recipient-starved cells in G0 led to shifts in the cell cycle. For example, ACH2 EVs appeared to arrest cells in the G2/M compared to CEM EVs where approximately 15.2% and 20.7% of CEM cells exposed to CEM and ACH2 EVs, respectively, were in G2/M (**Fig. 16-C**). Addition of ICAM-1 seemed to release this block reducing the number of cells in G2/M to 6.8% (**Fig. 16C-E**). In the myeloid setting (**Fig. 16F-K**), changes in cell cycle progression were minimal. Cell cycle block looked to be at the S phase. Approximately 12.6% of cell populations were in the S phase upon treatment with U937 EVs compared to 13% for U1 EVs whereas no change in G2/M populations were observed (**Fig. 16G-H**). ICAM-1 relieved the blockade at the S phase, increasing the number of cells in the G2/M phase from 2.1% to 3.5% (**Fig. 16I-K**). Together, these findings suggest that EVs affect cell cycle progression in recipient cells.

A)

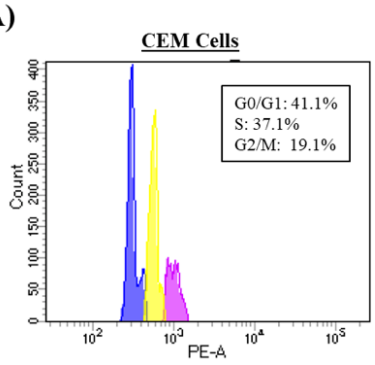
CEM Cells
G0/G1: 41.1%
S: 37.1%
G2/M: 19.1%
Count
PE-A

B)

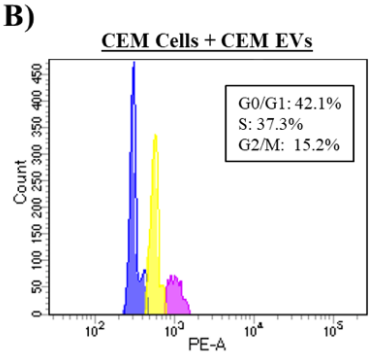
CEM Cells + CEM EVs
G0/G1: 42.1%
S: 37.3%
G2/M: 15.2%
Count
PE-A

C)

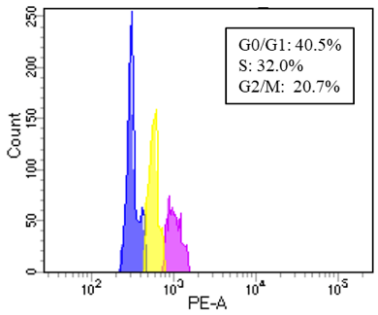
CEM Cells +ACH2 EVs
G0/G1: 40.5%
S: 32.0%
G2/M: 20.7%
Count
PE-A

D)

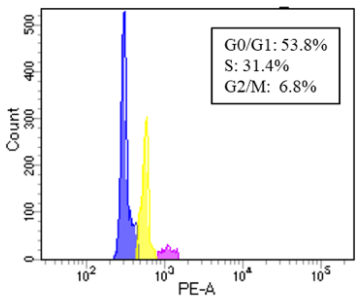
CEM Cells +ACH2 EVs +ICAM1
G0/G1: 53.8%
S: 31.4%
G2/M: 6.8%
Count
PE-A

E)

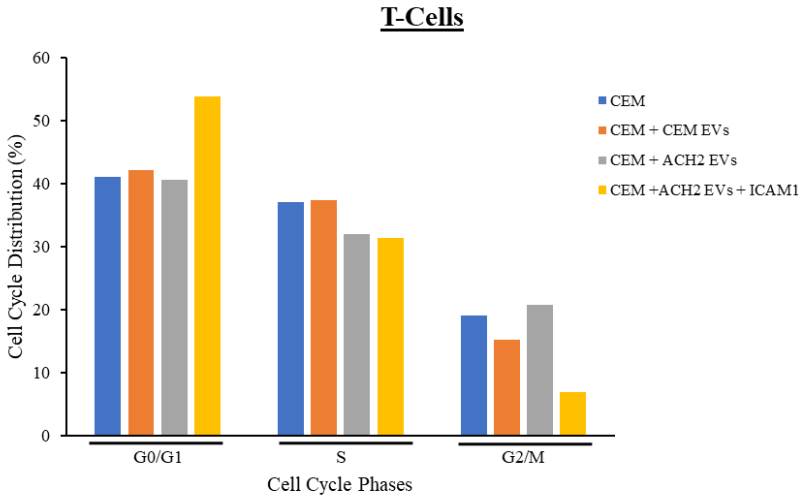
T-Cells
Cell Cycle Distribution (%)
Cell Cycle Phases
G0/G1
S
G2/M
CEM
CEM + CEM EVs
CEM + ACH2 EVs
CEM +ACH2 EVs + ICAM1

F)

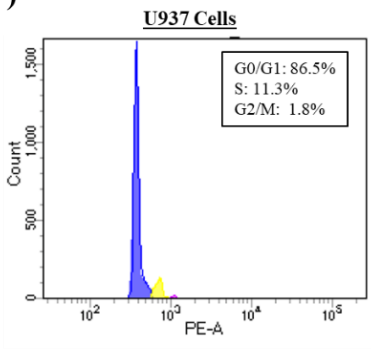
U937 Cells
G0/G1: 86.5%
S: 11.3%
G2/M: 1.8%
Count
PE-A

G)

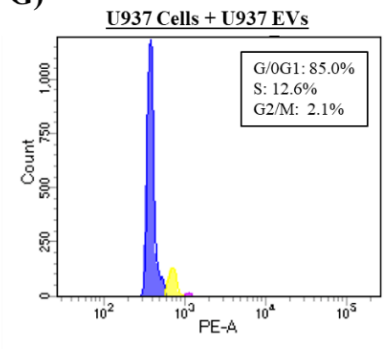
U937 Cells + U937 EVs
G/0G1: 85.0%
S: 12.6%
G2/M: 2.1%
Count
PE-A

H)

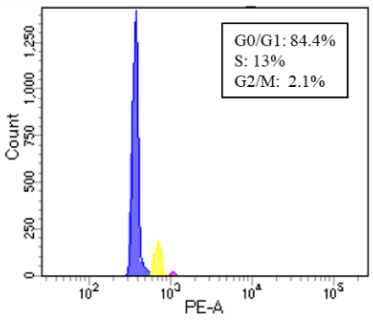
U937 Cells +U1 EVs
G0/G1: 84.4%
S: 13%
G2/M: 2.1%
Count
PE-A

I)

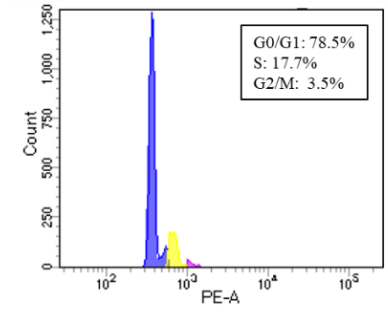
U937 Cells +U1 EVs +ICAM1
G0/G1: 78.5%
S: 17.7%
G2/M: 3.5%
Count
PE-A

J)

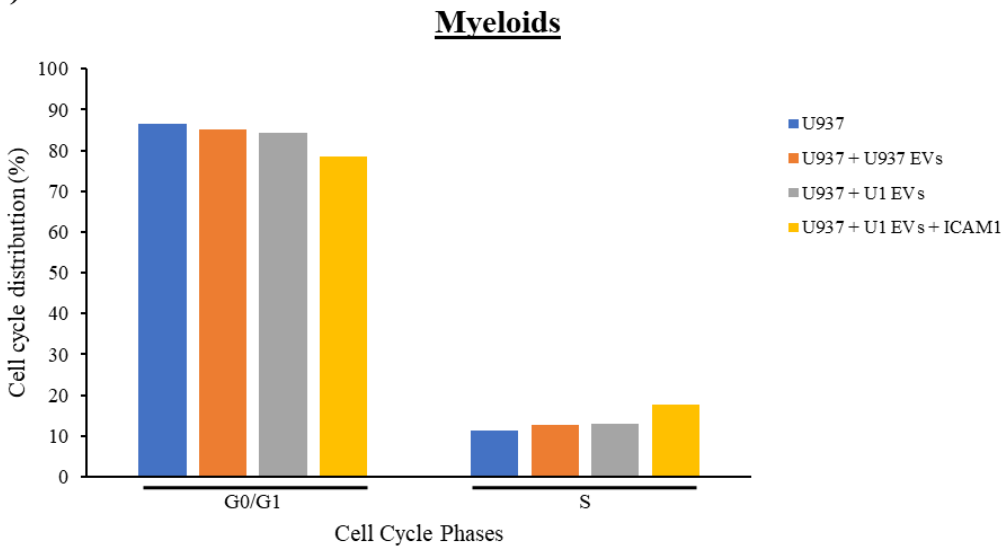
Myeloids
Cell cycle distribution (%)
G0/G1
S
Cell Cycle Phases
U937
U937 + U937 EVs
U937 + U1 EVs
U937 + U1 EVs + ICAM1

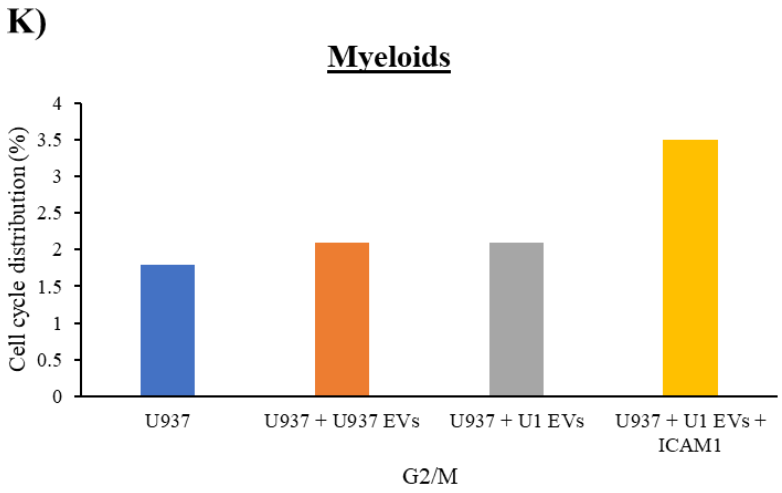

Figure 16: EVs modulate changes in the cell cycle dynamics of recipient cells. Cell cycle analysis of CEM cells (**A**) treated with CEM EVs (**B**), ACH2 EVs (**C**), and (**D**) ACH2 EVs and ICAM-1. Cell cycle analysis of U937 cells (**F**) treated with U937 EVs (**G**), U1 EVs (**H**), and (**I**) U1 EVs and ICAM-1. (**E, J-K**) Statistics of the cell cycle distribution.

CHAPTER FOUR: DISCUSSION

Extracellular vesicles (EVs) have been shown to be secreted by virtually all cell types and contain cargo such as nucleic acids, lipids, and proteins that are delivered to target cells and elicit functional changes in the recipient cells (13, 14, 89, 90). Furthermore, they have been implicated in mediating numerous disease pathogenesis including bacterial infections, cancer, viral infections, neurodegenerative disorders, cardiovascular diseases, and inflammatory diseases (22, 23, 83, 91–93). This clearly points to the undeniable role of EVs as regulators of intercellular communication. Recently, we have found that EVs derived from uninfected cells activate latent HIV-1 (33). However, the mechanism associated this event was unclear. This current study elucidates the mechanism behind the activation of latent HIV-1. Our data indicate that EVs from uninfected T-cells contain several kinases including c-Src. Upon the internalization of EVs, c-Src initiates a signal cascade which leads to the successive activation of EGFR, PI3K, AKT, mTOR, STAT3, and SRC-1, respectively. This ultimately leads to the increased loading of RNA Polymerase II onto the viral promoter, increasing transcription of HIV-1 (42). In addition, our data indicate that EVs derived from HIV-1infected-cells contain several kinases including CDK10, GSK3β, and MAPK8 that are differentially expressed compared to uninfected EVs. We found that these EV-associated kinases are biologically active and able to phosphorylate substrates such as histone H1. Importantly, we found that these kinases elicit functional changes in recipient cells, notably, in the cell cycle dynamics. These findings suggest that EVs play a critical in HIV-1 pathogenesis.

Kinases have been well documented as indispensable molecular switches that regulate several biological processes (94, 95). Similarly, EVs (via their cargo) have also been implicated in mediating various functions critical to cell survival including immune responses, cell survival, and cell differentiation (96). As such, it is not surprising that EV-associated kinases would stimulate changes in recipient cells. Data from this study indicated that kinases are present in extracellular vesicles. Specifically, several members of the Src family of kinases including Hck, Lck, c-Src, and Fyn were found to be enriched in EVs from uninfected T-cells (**Fig. 2**). The viral protein, Nef, has been shown to promote viral pathogenicity by altering signaling pathways through its interaction with c-Src at the SH3 domain (97). Results from Trible *et al*. demonstrated the direct activation of c-Src by Nef upon introduction of Nef in a yeast-based expression system (97). The activation of c-Src by Nef may result in the activation of the transcription factor STAT3 and ERK, thereby promoting cell survival (98, 99). Although, our current study shows and focuses on the role c-Src present in EVs derived from uninfected T-cells plays in propagating activation signals that leads to increased transcription of HIV-1, other members of the Src family of kinases such as Hck, Lck, and Fyn, all of which have been found to interact with various HIV-1 accessory proteins, could be involved in the activation of latent HIV-1 via different mechanisms. For instance, Hck which is expressed primarily in myeloid cells, has been shown to be activated by the viral protein Nef via the interaction of its proline-rich motif with the Hck SH3 domain (38). A study performed by Lee *et. al* reported that EVs isolated from the plasma of HIV-1 patients contained Hck (39). The authors found that the Nef-mediated activation of Hck prompted

the activation and packaging of ADAM17, the sheddase of TNF, into plasma EVs (39). This could potentially contribute to the progression of viral infection by altering immune responses stemming from the release of TNF. Similarly, Lck has been shown to be activated following HIV-1 infection, packaged into the HIV-1 virion, and involved in the reactivation of latent HIV-1 following T-cell stimulation (100, 101). Lck contributes to HIV-1 pathogenesis by physically interacting with the viral protein Gag and directing it to the plasma membrane, thus promoting viral assembly and egress (101). Furthermore, T-cells lacking Lck were shown to accumulate HIV-1 intracellularly while HeLa cells constructed to overexpress Lck had increased Gag plasma membrane localization, lending further evidence of Lck's role in viral maturation (101). Lastly, the deregulation of Fyn activity which mediates T-cell activation, has been implicated in immune system failures associated with HIV-1 infection. This was proven by the increased kinase activity of Fyn upon treatment with viral gp120-derived peptides in peripheral blood lymphoblasts (102). Phipps *et al.* reported that within seconds of HIV-1 infection, Fyn initiates a signal cascade that results in T-cell activation (103). Their data showed that HIV-1 patients who were asymptomatic had a 19-fold increase in Fyn kinase activity compared to the healthy controls (103). On the other hand, Fyn activity of former HIV-1 patients who had advanced to AIDS was less affected (increase of 3-fold), suggesting that Fyn kinase activity could be a diagnostic indicator for early infection or a prognostic marker for AIDS advancement (103). Collectively, these point to the possibility of EV-associated Hck, Lck, and Fyn as additional mediators of the activation of latent HIV-1. Further studies are needed to investigate this intriguing prospect.

Data from this study strongly suggest that EV-associated kinases are biologically active and capable of phosphorylating substrates, leading to functional changes in recipient cells (**Fig. 4, 14, 16**). This is especially important in the context of the effectiveness of cART in sanctuary sites such as the brain. Unlike cART, exosomes can cross the blood-brain barrier, which is made up of brain endothelial cells that act as a filter restricting the movement of substances between the brain and circulation, and stimulate brain cells including microglia – the main HIV-1 reservoir in the brain (104, 105). Hence, EVs containing functional kinases could perhaps stimulate viral transcription in microglial cells and promote the production of pro-inflammatory cytokines, which could in turn lead to neuroinflammation, a hallmark characteristic of HAND. This could explain clinical findings where when activated, microglial cells secrete several neurotoxic host factors such as cytokines (TNFα, IFNα, IL6, IL8, IL1β) and chemokines (CCL2, CCL5) (106). In fact, a study exploring the gene expression profile in microglial cells derived from HIV-1 encephalitis patients on cART found altered expression of proinflammatory cytokines IL-1β and IL-6 compared to uninfected patients (107). Therefore, EV-associated kinases could potentially contribute to HIV-1 pathogenesis by stimulating microglial cells via activating certain substrates and signal pathways.

In this study, we also found that the EV activation of latent HIV-1 occurs via the PI3K/AKT/mTOR pathway (**Fig. 6, 8-9**). This pathway mediates several biological processes including cell survival, metabolism, proliferation, and growth (108). Others have shown that HIV-1 protein Nef promotes the establishment of viral latency by

interacting with PI3K and AKT, inducing anti-apoptotic signals and dampening immune responses (109, 110). This is in line with data from this study that demonstrate that activation of the PI3K/AKT/mTOR pathway by EV-associated c-Src affects viral pathogenesis. Additionally, the inhibition of various proteins by kinase inhibitors resulted in decreased levels of TAR RNA and genomic RNA (**Fig. 6A-B**). The extent of the reduction significantly differed across members of our proposed signal pathway (i.e., c-Src, EGFR, PI3K, AKT-1, mTOR, STAT3, SRC-1), suggesting additional EV titration studies may be needed and/or there may be alternative mechanisms that could also lead to activation of HIV-1 transcription. The Ras-MAPK/ERK pathway could be a potential alternative route utilized by c-Src to increase the transcription of HIV-1. Studies have shown the Ras-MAPK/ERK signaling pathway, which is involved in cell proliferation and differentiation, is activated by c-Src (111–113). In the context of HIV-1 pathogenesis, Yang *et al*. reported that the infectivity of HIV-1 was improved by the activation of the MAPK/ERK pathway via the phosphorylation and activation of Vif (114, 115). This points to the possibility of the Ras-MAPK/ERK pathway as an alternate pathway (in addition to the PI3K/AKT/mTOR pathway) that could lead to enhanced HIV-1 replication.

The latter part of this study focused on examining the contents and effects of EVs released from HIV-1-infected cells on recipient cells. Our kinome profiling of EVs derived from uninfected and HIV-1infected cells revealed over 180 kinases present. Based on the differential expression, association to HIV-1 pathogenesis, and statistical significance, we selected 3 kinases (CDK10, GSK3β, and MAPK8) for further analysis

(**Fig. 11**). While this process we used to identify and prioritize a few EV-associated kinases could have inadvertently eliminated numerous worthy candidates that are also instrumental in HIV-1 transcription, this strategy yielded promising discoveries – some of which will be addressed in future works. Nevertheless, our results from this current manuscript are in line with other studies that have shown that the contents of EVs derived from HIV-1-infected cells contain several unique host molecules in comparison to EVs from uninfected cells (23, 29, 72). Selective packaging of specific molecules into HIV-1-infected EVs is most likely advantageous to the survival and spread of the virus. For instance, by interfering with the integrity of the function of antiviral immune cells to increase the susceptibility of naïve cells to infection. Data from **Fig. 11-12** demonstrate that CDK10, GSK3β, and MAPK8 are upregulated in ACH2 and U1 EVs in comparison to their uninfected counterparts (i.e., CEM and U937). This differential expression could explain our results in **Fig. 14** where we observed that histone H1 was phosphorylated with our 3 kinases of interests from mostly the HIV-1-infected EVs, ACH2 and U1. Furthermore, it should be noted that these EV-associated kinases may be part of a larger complex. In the past, we have found multiple distinct CDK9/T1 complexes (crucial in HV-1 transcription elongation) in T-cells (116). One of these CDK9/T1 complexes was present only in HIV-1-infected cells and extremely sensitive to treatment with a CDK inhibitor known as CR8#13 (116). This could partly explain the differential expression of EV-associated kinases derived from HIV-1 infected cells versus uninfected cells we observed in this current study, where unique protein complexes may exist only in EVs

derived from HIV-1 infected cells and contributing to the differential expression of these kinases.

The ability of EV-associated CDK10, GSK3β, and MAPK8 to phosphorylate and activate substrates could result in signal transductions that lead to enhanced viral replication. All these kinases are present in the cell and mediate gene expression in response to various stimuli. Kinases from HIV-1-infected EVs could serve as a stimulus to trigger changes in the target cell. Data in **Fig. 13** suggests that EVs from HIV-1-infected cells are internalized at a faster rate and greater amounts compared to uninfected EVs. Moreover, these HIV-1-infected EVs contain upregulated levels of these kinases (**Fig. 12A**) and a higher phosphorylation activity of substrates (**Fig. 14A-B**). These point to the possibility that EV-associated kinases entering the cell could jump-start the signal transduction process by activating cellular substrates. Retained activation could lead to phenotypic changes that are advantageous to viral spread. For instance, the MAPK pathway, of which MAPK8 is a part of, has been shown to be activated by HIV-1 proteins Vpr, Tat, Nef, and gp120 in microglia and astrocytes to intensify the host inflammatory response, ultimately compromising the integrity of the BBB (117, 118). The MAPK pathway has also been implicated in regulating the AP-1 transcription factors c-Fos and c-Jun, which activate HIV-1 transcription by binding to the viral promoter and recruiting the SWI/SNF chromatin remodeling complex (45, 119–121). Originally thought of as a kinase that only regulates metabolism, experimental evidence has demonstrated the role of GSK3β in several biological processes such as cell division, embryonic development, apoptosis, and microtubule function (122). In the context of

HIV-1, GSK3β modulates the functions of transcription factors and cofactors that are essential for viral transcription including β-catenin, c-Jun, c-Myc, C/EBPα/β, NFATc, RelA, and CREB (123–125). Along the same lines, CDK10 controls the activity of the transcription factor ETS2, which has been shown to regulate HIV-1 latency by repressing viral transcription via binding to a repressor–activator target sequence of the viral 5′-LTR (43, 126). In all, the convergence of these EV-associated kinases (i.e., MAPK8, GSK3β, and CDK10) may result in changes in a number of signaling pathways, as well as the level and functional properties of various cellular transcription factors. This could ultimately modify the course of the viral promoter, leading to increased gene expression and HIV-1 pathogenesis.

In this study, we provide experimental evidence that shows modifications in the cell cycle dynamics of cells treated with EVs from both uninfected and HIV-1-infected cells. The cell cycle is integral to HIV-1 replication. This is because HIV-1 requires host cell machinery for replication – some of which are only available at certain phases of the cell cycle. Furthermore, Vif and Vpr, which have both been shown to be present in EVs derived from urine samples of HIV-1 patients under cART, have been shown to cause cell cycle arrest at the G2 phase (127–129). In T-cells, HIV-1 via Vpr, induces cell cycle arrest or delay in the G2 phase, blocking proliferation of infected cells (127). This was found to be advantageous to the virus because expression of the viral genome is at its peak during the G2 phase. Thus, the HIV-1 maximizes virus production during this phase of the cell cycle to keep up with the destruction of infected cells by the host immune system (127). Mechanistically, Vpr was found to arrest the cell cycle at G2 by preventing

the activation of CDC2/CDK1, a kinase that regulates the G2/M checkpoint (126, 130). Similarly, Wang *et al.* reported that viral accessory protein Vif also causes G2 arrest (131). The authors demonstrated that Vif interacts with host factor, CDK9, which is known to work in normal cell cycle control and is also a component of the transcription regulator, P-TEFb (128). This interaction was confirmed with siRNA experiments where knockdown of CDK9 in Vif-transfected HeLa cells prevented the early transition of G1 to S phase (128). Together, these results are in line with the data presented in this study where we found that the addition of HIV-1-infected ACH2 EVs to serum-starved recipient cells led to progression in the cell cycle and arrest at the G2/M phase (**Fig. 16**). This could perhaps be due to the increased expression of CDK10, a kinase that is related to CDC2 (regulator of the G2/M checkpoint) and phylogenetically similar to CDK9 (132), in these infected EVs. The involvement of CDK10, MAPK8, and GSK3β in modifying cell cycle dynamics, EV release, and virion production in recipient cells will be further confirmed in future studies using a pharmacological perturbation approach where EVs will be isolated from cells treated with different concentrations of various kinase inhibitors including NVP-2 (inhibitor against CDK10), AZD2858 (inhibitor against GSK3β), and DB07268 (inhibitor against MAPK8) (**Supplemental Fig. 1**); and used to treat recipient cells.

In summary, the current cART regimen does not contain an FDA-approved transcription inhibitor. As such, cART can be improved by targeting viral transcription and preventing the translation of HIV-1 proteins. Data from this study demonstrate that EVs, via their kinase cargo, activate viral transcription by initiating signaling cascades.

This increased transcription could result in amplified virus production as well as upregulation of viral proteins. This could lead to the dysfunction of cellular processes related to immune response and cell cycle control, thereby resulting in enhanced viral spread, production of toxic metabolites, and complications such as HAND. Our data suggest that targeting EV-associated CDK10, MAPK8, and GSK3β using a pharmacological perturbation approach could potentially mitigate this process. This is because the 3 aforementioned kinases are positioned at the nexus of several signaling pathways essential to HIV-1 transcription including the PI3K/AKT, MAPK, and NF-κB pathways (40, 43, 45, 124). Hence, the use of this tactic of curbing viral transcription is not too far-fetched as kinases make up a significant portion of recognized drug targets, thereby making them one of the most important drug targets of this century (133). Small-molecule kinase inhibitors have been successfully utilized in the field of cancer to improve patient outcomes. As such, future studies will focus on the use of NVP-2, DB07268, and AZD2858 kinase inhibitors against CDK10, MAPK8, and GSK3β, respectively, to curb viral transcription and restore normal cell cycle control in HIV-1-latently infected cells. Future experiments will examine whether these small-molecule kinase inhibitors work synergistically with cART in reducing viral replication. We will also validate the efficacy of our kinase inhibitors using tools such as siRNA and shRNA related treatments against specific kinases to address specificity issues that may arise with our small-molecule kinase inhibitors. Lastly, because our EV kinome profiling revealed the presence and differential expression of several other kinases, additional efforts will go toward investigating and confirming alternative kinases within EVs that could also lead

to changes in viral transcription. Additional methods such as reverse phase protein microarrays (RPPA), which can shed light on the phosphorylation status of proteins involved in a signal pathway, will also be used to further examine kinase networks (134–136).

Overall, this study has demonstrated that uninfected and infected EVs contain functionally active kinases that mediate functional changes in recipient cells. These functional changes include increased HIV-1 transcription and changes in cell cycle dynamics. Several kinases derived from HIV-1-infected cells were found to be differentially expressed compared to those from uninfected cells, potentially contributing to enhanced viral replication. As summarized in **Fig. 17**, the uptake of EVs containing biologically active kinases by recipient cells could initiate a signal cascade that may result in changes in the levels of various cellular transcription factors and activation of the viral promoter, ultimately giving rise to increased transcription of viral genes and HIV-1 pathogenesis. These findings could improve our understanding of the mechanisms underlying HIV-1 latency and serve as the basis for uncovering effective therapeutic targets.

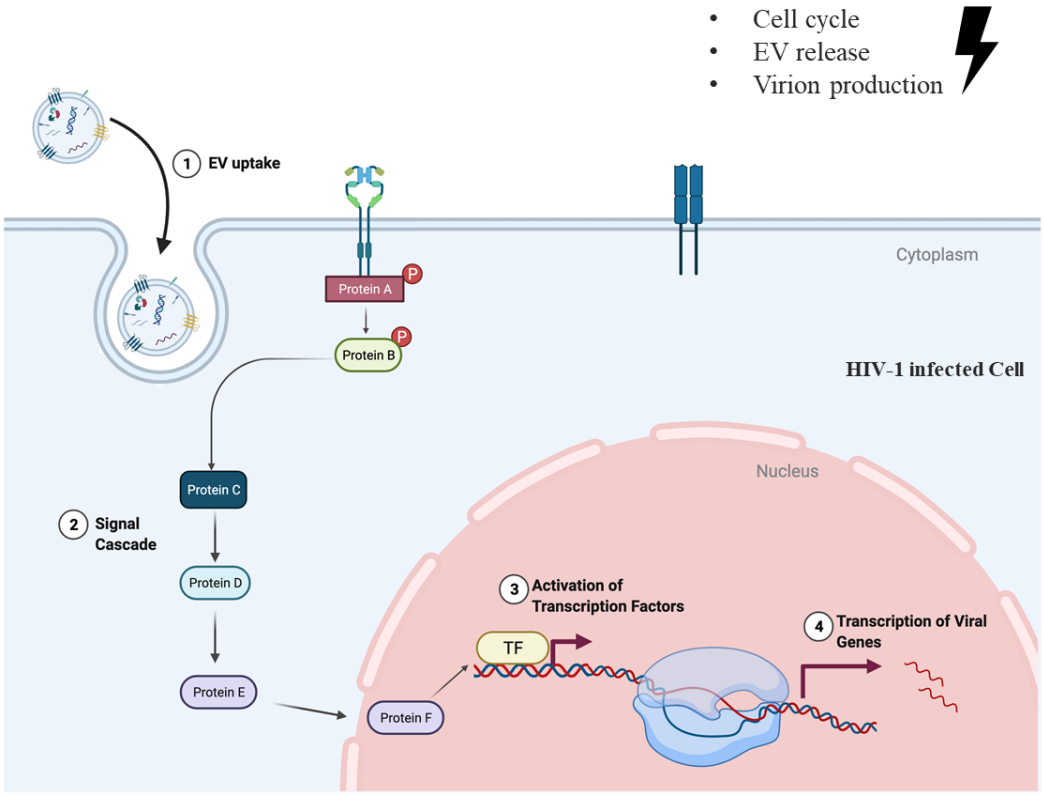

Figure 17: Effects of EV-associated kinases on HIV-1 pathogenesis. EVs containing kinases are taken up by recipient cells resulting in changes in the activation of signaling pathways, as well as changes in the levels and functional properties of various cellular transcription factors. This could ultimately modify the course of the viral promoter, leading to increased gene expression and HIV-1 pathogenesis.

CHAPTER FIVE: SUPPLEMENTAL FIGURES

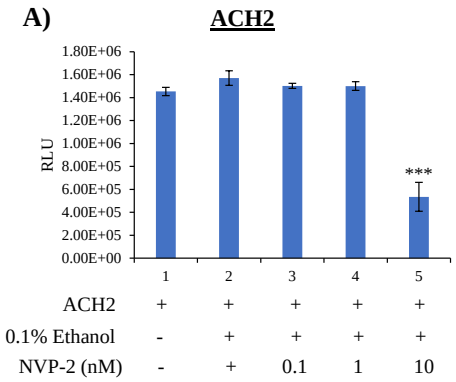

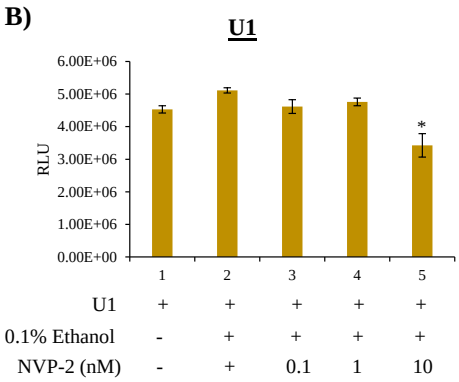

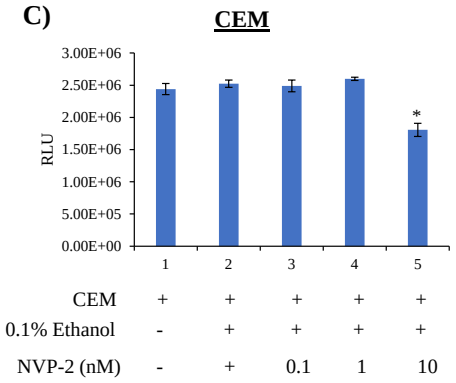

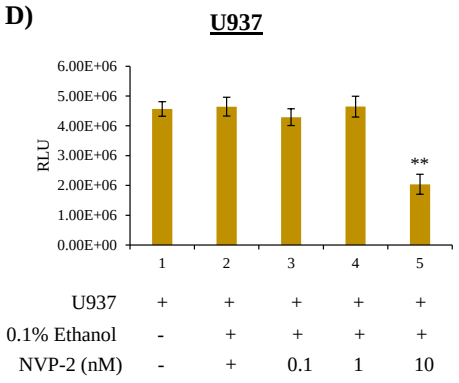

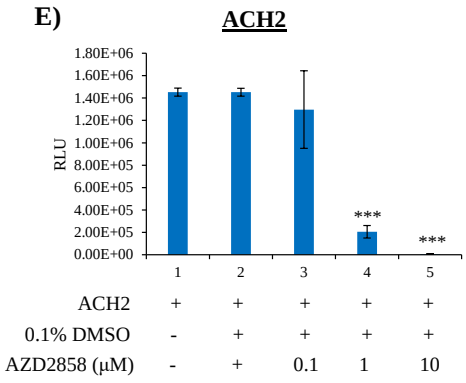

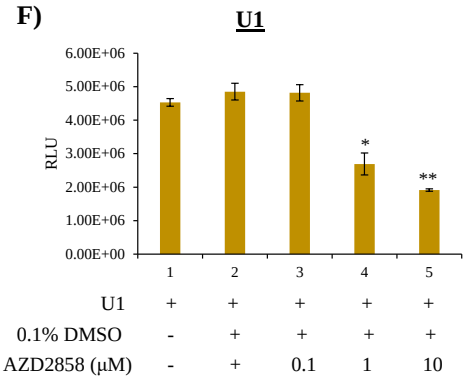

G) **CEM**

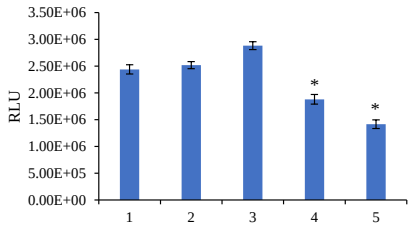

CEM	+	+	+	+	+
0.1% DMSO	-	+	+	+	+
AZD2858 (µM)	-	+	0.1	1	10

H) **U937**

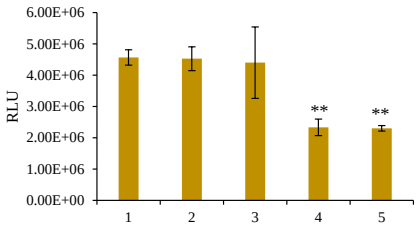

U937	+	+	+	+	+
0.1% DMSO	-	+	+	+	+
AZD2858 (µM)	-	+	0.1	1	10

I) **ACH2**

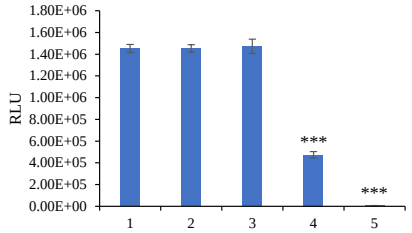

ACH2	+	+	+	+	+
0.1% DMSO	-	+	+	+	+
DB07268 (µM)	-	+	0.1	1	10

J) **U1**

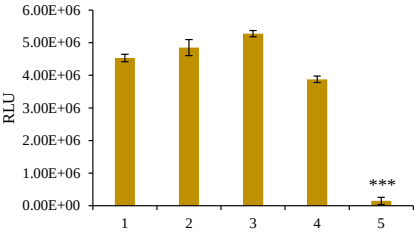

U1	+	+	+	+	+
0.1% DMSO	-	+	+	+	+
DB07268 (µM)	-	+	0.1	1	10

K) **CEM**

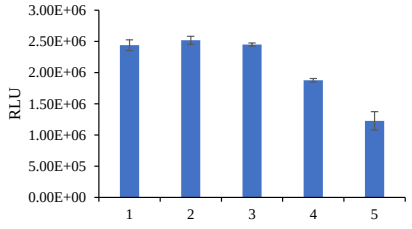

CEM	+	+	+	+	+
0.1% DMSO	-	+	+	+	+
DB07268 (µM)	-	+	0.1	1	10

L) **U937**

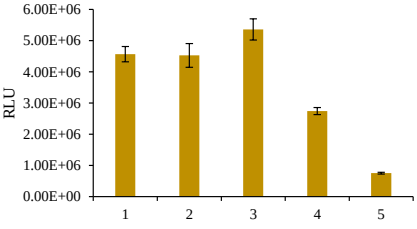

U937	+	+	+	+	+
0.1% DMSO	-	+	+	+	+
DB07268 (µM)	-	+	0.1	1	10

Supplemental Figure 1: Cell viability for CDK10, GSK3β, and MAPK8 kinase inhibitors. CEM, ACH2, U937, and U1 cells (5×10^4) were plated with various concentrations of kinase inhibitors and allowed to incubate for 48 hours followed by a cell viability assay. (**A**) ACH2 cells treated with NVP-2 (CDK10 inhibitor). (**B**) U1 cells treated with NVP-2 (CDK10 inhibitor). (**C**) CEM cells treated with NVP-2 (CDK10 inhibitor). (**D**) U937cells treated NVP-2 (CDK10 inhibitor). (**E**) ACH2 cells treated with AZD2858 (GSK3β inhibitor). (**F**) U1 cells treated with AZD2858 (GSK3β inhibitor). (**G**) CEM cells treated with AZD2858 (GSK3β inhibitor). (**H**) U937cells treated AZD2858 (GSK3β inhibitor). (**I**) ACH2 cells treated with DB07268 (MAPK8 inhibitor). (**J**) U1 cells treated with DB07268 (MAPK8 inhibitor). (**K**) CEM cells treated with DB07268 (MAPK8 inhibitor). (**L**) U937cells treated DB07268 (MAPK8 inhibitor). Error bars represent ± S.D. of three technical replicates for all panels. A two-tailed Student's t-test was used to assess significance: *$p < 0.05$; **$p < 0.01$; ***$p < 0.001$.

REFERENCES

1. HIV/AIDS [online] https://www.who.int/westernpacific/health-topics/hiv-aids (Accessed November 6, 2021)
2. Statistics Overview | Statistics Center | HIV/AIDS | CDC (2021) [online] https://www.cdc.gov/hiv/statistics/overview/index.html (Accessed July 27, 2021)
3. The Burden of HIV: Insights From the Global Burden of Disease Study 2010 - PubMed [online] https://pubmed.ncbi.nlm.nih.gov/23660576-the-burden-of-hiv-insights-from-the-global-burden-of-disease-study-2010/ (Accessed December 1, 2019)
4. Pau, A. K., and George, J. M. (2014) Antiretroviral Therapy: Current Drugs. *Infect. Dis. Clin. North Am.* **28**, 371–402
5. HIV-associated neurocognitive disorders persist in the era of potent antiretroviral therapy [online] https://www.ncbi.nlm.nih.gov/pmc/articles/PMC2995535/ (Accessed December 1, 2019)
6. Kumar, A. M., Borodowsky, I., Fernandez, B., Gonzalez, L., and Kumar, M. (2007) Human immunodeficiency virus type 1 RNA Levels in different regions of human brain: quantification using real-time reverse transcriptase-polymerase chain reaction. *J. Neurovirol.* **13**, 210–224
7. Hatano, H., Jain, V., Hunt, P. W., Lee, T.-H., Sinclair, E., Do, T. D., Hoh, R., Martin, J. N., McCune, J. M., Hecht, F., Busch, M. P., and Deeks, S. G. (2013) Cell-based measures of viral persistence are associated with immune activation and programmed cell death protein 1 (PD-1)-expressing CD4+ T cells. *J. Infect. Dis.* **208**, 50–56
8. Kumar, A., Abbas, W., and Herbein, G. (2014) HIV-1 Latency in Monocytes/Macrophages. *Viruses*. **6**, 1837–1860
9. Dornadula, G., Zhang, H., VanUitert, B., Stern, J., Livornese, J., Lawrence, Ingerman, M. J., Witek, J., Kedanis, R. J., Natkin, J., DeSimone, J., and Pomerantz, R. J. (1999) Residual HIV-1 RNA in Blood Plasma of Patients Taking Suppressive Highly Active Antiretroviral Therapy. *JAMA*. **282**, 1627–1632
10. Günthard, H. F., Havlir, D. V., Fiscus, S., Zhang, Z.-Q., Eron, J., Mellors, J., Gulick, R., Frost, S. D. W., Brown, A. J. L., Schleif, W., Valentine, F., Jonas, L., Meibohm, A., Ignacio, C. C., Isaacs, R., Gamagami, R., Emini, E., Haase, A., Richman, D. D., and Wong, J. K. (2001) Residual Human Immunodeficiency Virus (HIV) Type 1 RNA and DNA in Lymph Nodes and HIV RNA in Genital Secretions and in Cerebrospinal Fluid after Suppression of Viremia for 2 Years. *J. Infect. Dis.* **183**, 1318–1327
11. Ishizaka, A., Sato, H., Nakamura, H., Koga, M., Kikuchi, T., Hosoya, N., Koibuchi, T., Nomoto, A., Kawana-Tachikawa, A., and Mizutani, T. (2016) Short Intracellular HIV-1 Transcripts as Biomarkers of Residual Immune Activation in Patients on Antiretroviral Therapy. *J. Virol.* **90**, 5665–5676

12. Imamichi, H., Dewar, R. L., Adelsberger, J. W., Rehm, C. A., O'Doherty, U., Paxinos, E. E., Fauci, A. S., and Lane, H. C. (2016) Defective HIV-1 proviruses produce novel protein-coding RNA species in HIV-infected patients on combination antiretroviral therapy. *Proc. Natl. Acad. Sci. U. S. A.* **113**, 8783–8788
13. Dias, M. V. S., Costa, C. S., and daSilva, L. L. P. (2018) The Ambiguous Roles of Extracellular Vesicles in HIV Replication and Pathogenesis. *Front. Microbiol.* 10.3389/fmicb.2018.02411
14. H Rashed, M., Bayraktar, E., K Helal, G., Abd-Ellah, M. F., Amero, P., Chavez-Reyes, A., and Rodriguez-Aguayo, C. (2017) Exosomes: From Garbage Bins to Promising Therapeutic Targets. *Int. J. Mol. Sci.* 10.3390/ijms18030538
15. Doyle, L. M., and Wang, M. Z. (2019) Overview of Extracellular Vesicles, Their Origin, Composition, Purpose, and Methods for Exosome Isolation and Analysis. *Cells*. **8**, 727
16. Johnstone, R. M., Mathew, A., Mason, A. B., and Teng, K. (1991) Exosome formation during maturation of mammalian and avian reticulocytes: Evidence that exosome release is a major route for externalization of obsolete membrane proteins. *J. Cell. Physiol.* **147**, 27–36
17. Simeone, P., Bologna, G., Lanuti, P., Pierdomenico, L., Guagnano, M. T., Pieragostino, D., Del Boccio, P., Vergara, D., Marchisio, M., Miscia, S., and Mariani-Costantini, R. (2020) Extracellular Vesicles as Signaling Mediators and Disease Biomarkers across Biological Barriers. *Int. J. Mol. Sci.* **21**, 2514
18. Clancy, J. W., Boomgarden, A. C., and D'Souza-Schorey, C. (2021) Profiling and promise of supermeres. *Nat. Cell Biol.* **23**, 1217–1219
19. Zhang, H., and Lyden, D. (2019) Asymmetric flow field-flow fractionation technology for exomere and small extracellular vesicle separation and characterization. *Nat. Protoc.* **14**, 1027–1053
20. Brennan, K., Martin, K., FitzGerald, S. P., O'Sullivan, J., Wu, Y., Blanco, A., Richardson, C., and Mc Gee, M. M. (2020) A comparison of methods for the isolation and separation of extracellular vesicles from protein and lipid particles in human serum. *Sci. Rep.* **10**, 1039
21. Yuan, Q., Li, X., Zhang, S., Wang, H., and Wang, Y. (2021) Extracellular vesicles in neurodegenerative diseases: Insights and new perspectives. *Genes Dis.* **8**, 124–132
22. Fu, S., Zhang, Y., Li, Y., Luo, L., Zhao, Y., and Yao, Y. (2020) Extracellular vesicles in cardiovascular diseases. *Cell Death Discov.* **6**, 1–9
23. Sampey, G. C., Saifuddin, M., Schwab, A., Barclay, R., Punya, S., Chung, M.-C., Hakami, R. M., Asad Zadeh, M., Lepene, B., Klase, Z. A., El-Hage, N., Young, M., Iordanskiy, S., and Kashanchi, F. (2016) Exosomes from HIV-1-infected Cells Stimulate Production of Pro-inflammatory Cytokines through Trans-activating Response (TAR) RNA. *J. Biol. Chem.* **291**, 1251–1266
24. Alem, F., Olanrewaju, A. A., Omole, S., Hobbs, H. E., Ahsan, N., Matulis, G., Brantner, C. A., Zhou, W., Petricoin, E. F., Liotta, L. A., Caputi, M., Bavari, S., Wu, Y., Kashanchi, F., and Hakami, R. M. (2021) Exosomes originating from infection with the cytoplasmic single-stranded RNA virus Rift Valley fever virus

(RVFV) protect recipient cells by inducing RIG-I mediated IFN-B response that leads to activation of autophagy. *Cell Biosci.* **11**, 220
25. Martínez-Rojas, P. P., Quiroz-García, E., Monroy-Martínez, V., Agredano-Moreno, L. T., Jiménez-García, L. F., and Ruiz-Ordaz, B. H. (2020) Participation of Extracellular Vesicles from Zika-Virus-Infected Mosquito Cells in the Modification of Naïve Cells' Behavior by Mediating Cell-to-Cell Transmission of Viral Elements. *Cells*. **9**, E123
26. Pleet, M. L., Mathiesen, A., DeMarino, C., Akpamagbo, Y. A., Barclay, R. A., Schwab, A., Iordanskiy, S., Sampey, G. C., Lepene, B., Ilinykh, P. A., Bukreyev, A., Nekhai, S., Aman, M. J., and Kashanchi, F. (2016) Ebola VP40 in Exosomes Can Cause Immune Cell Dysfunction. *Front. Microbiol.* 10.3389/fmicb.2016.01765
27. Anand, S., Samuel, M., Kumar, S., and Mathivanan, S. (2019) Ticket to a bubble ride: Cargo sorting into exosomes and extracellular vesicles. *Biochim. Biophys. Acta BBA - Proteins Proteomics*. **1867**, 140203
28. Narayanan, A., Iordanskiy, S., Das, R., Van Duyne, R., Santos, S., Jaworski, E., Guendel, I., Sampey, G., Dalby, E., Iglesias-Ussel, M., Popratiloff, A., Hakami, R., Kehn-Hall, K., Young, M., Subra, C., Gilbert, C., Bailey, C., Romerio, F., and Kashanchi, F. (2013) Exosomes Derived from HIV-1-infected Cells Contain Trans-activation Response Element RNA. *J. Biol. Chem.* **288**, 20014–20033
29. Narayanan, A., Iordanskiy, S., Das, R., Van Duyne, R., Santos, S., Jaworski, E., Guendel, I., Sampey, G., Dalby, E., Iglesias-Ussel, M., Popratiloff, A., Hakami, R., Kehn-Hall, K., Young, M., Subra, C., Gilbert, C., Bailey, C., Romerio, F., and Kashanchi, F. (2013) Exosomes derived from HIV-1-infected cells contain trans-activation response element RNA. *J. Biol. Chem.* **288**, 20014–20033
30. Mack, M., Kleinschmidt, A., Brühl, H., Klier, C., Nelson, P. J., Cihak, J., Plachý, J., Stangassinger, M., Erfle, V., and Schlöndorff, D. (2000) Transfer of the chemokine receptor CCR5 between cells by membrane-derived microparticles: a mechanism for cellular human immunodeficiency virus 1 infection. *Nat. Med.* **6**, 769–775
31. Rozmyslowicz, T., Majka, M., Kijowski, J., Murphy, S. L., Conover, D. O., Poncz, M., Ratajczak, J., Gaulton, G. N., and Ratajczak, M. Z. (2003) Platelet- and megakaryocyte-derived microparticles transfer CXCR4 receptor to CXCR4-null cells and make them susceptible to infection by X4-HIV. *AIDS Lond. Engl.* **17**, 33–42
32. Altan-Bonnet, N. (2016) Extracellular vesicles are the Trojan horses of viral infection. *Curr. Opin. Microbiol.* **32**, 77–81
33. Barclay, R. A., Schwab, A., DeMarino, C., Akpamagbo, Y., Lepene, B., Kassaye, S., Iordanskiy, S., and Kashanchi, F. (2017) Exosomes from uninfected cells activate transcription of latent HIV-1. *J. Biol. Chem.* **292**, 11682–11701
34. Cheng, H.-C., Qi, R. Z., Paudel, H., and Zhu, H.-J. (2011) Regulation and Function of Protein Kinases and Phosphatases. *Enzyme Res.* **2011**, 794089
35. Kannaiyan, R., and Mahadevan, D. (2018) A comprehensive review of protein kinase inhibitors for cancer therapy. *Expert Rev. Anticancer Ther.* **18**, 1249–1270
36. Ferguson, F. M., and Gray, N. S. (2018) Kinase inhibitors: the road ahead. *Nat. Rev. Drug Discov.* **17**, 353–377

37. Hamada, K., Maeda, Y., Mizutani, A., and Okada, S. (2019) The Phosphatidylinositol 3-Kinase p110α/PTEN Signaling Pathway Is Crucial for HIV-1 Entry. *Biol. Pharm. Bull.* **42**, 130–138
38. Saksela, K., Cheng, G., and Baltimore, D. (1995) Proline-rich (PxxP) motifs in HIV-1 Nef bind to SH3 domains of a subset of Src kinases and are required for the enhanced growth of Nef+ viruses but not for down-regulation of CD4. *EMBO J.* **14**, 484–491
39. Lee, J.-H., Ostalecki, C., Zhao, Z., Kesti, T., Bruns, H., Simon, B., Harrer, T., Saksela, K., and Baur, A. S. (2018) HIV Activates the Tyrosine Kinase Hck to Secrete ADAM Protease-Containing Extracellular Vesicles. *EBioMedicine*. **28**, 151–161
40. Wolschendorf, F., Bosque, A., Shishido, T., Duverger, A., Jones, J., Planelles, V., and Kutsch, O. (2012) Kinase Control Prevents HIV-1 Reactivation in Spite of High Levels of Induced NF-κB Activity. *J. Virol.* **86**, 4548–4558
41. Amata, I., Maffei, M., and Pons, M. (2014) Phosphorylation of unique domains of Src family kinases. *Front. Genet.* 10.3389/fgene.2014.00181
42. Barclay, R. A., Mensah, G. A., Cowen, M., DeMarino, C., Kim, Y., Pinto, D. O., Erickson, J., and Kashanchi, F. (2020) Extracellular Vesicle Activation of Latent HIV-1 Is Driven by EV-Associated c-Src and Cellular SRC-1 via the PI3K/AKT/mTOR Pathway. *Viruses*. 10.3390/v12060665
43. Kasten, M., and Giordano, A. (2001) Cdk10, a Cdc2-related kinase, associates with the Ets2 transcription factor and modulates its transactivation activity. *Oncogene*. **20**, 1832–1838
44. Kehn-Hall, K., Guendel, I., Carpio, L., Skaltsounis, L., Meijer, L., Al-Harthi, L., Steiner, J. P., Nath, A., Kutsch, O., and Kashanchi, F. (2011) Inhibition of Tat-mediated HIV-1 replication and neurotoxicity by novel GSK3-beta inhibitors. *Virology*. **415**, 56–68
45. Liu, R., Lin, Y., Jia, R., Geng, Y., Liang, C., Tan, J., and Qiao, W. (2014) HIV-1 Vpr stimulates NF-κB and AP-1 signaling by activating TAK1. *Retrovirology*. **11**, 45
46. Emerman, M. (1996) HIV-1, Vpr and the cell cycle. *Curr. Biol.* **6**, 1096–1103
47. Hrecka, K., Gierszewska, M., Srivastava, S., Kozaczkiewicz, L., Swanson, S. K., Florens, L., Washburn, M. P., and Skowronski, J. (2007) Lentiviral Vpr usurps Cul4–DDB1[VprBP] E3 ubiquitin ligase to modulate cell cycle. *Proc. Natl. Acad. Sci.* **104**, 11778–11783
48. Pinto, D. O., DeMarino, C., Pleet, M. L., Cowen, M., Branscome, H., Al Sharif, S., Jones, J., Dutartre, H., Lepene, B., Liotta, L. A., Mahieux, R., and Kashanchi, F. (2019) HTLV-1 Extracellular Vesicles Promote Cell-to-Cell Contact. *Front. Microbiol.* 10.3389/fmicb.2019.02147
49. DeMarino, C., Pleet, M. L., Cowen, M., Barclay, R. A., Akpamagbo, Y., Erickson, J., Ndembe, N., Charurat, M., Jumare, J., Bwala, S., Alabi, P., Hogan, M., Gupta, A., Hooten, N. N., Evans, M. K., Lepene, B., Zhou, W., Caputi, M., Romerio, F., Royal, W., El-Hage, N., Liotta, L. A., and Kashanchi, F. (2018) Antiretroviral

Drugs Alter the Content of Extracellular Vesicles from HIV-1-Infected Cells. *Sci. Rep.* 10.1038/s41598-018-25943-2
50. Duverger, A., Wolschendorf, F., Anderson, J. C., Wagner, F., Bosque, A., Shishido, T., Jones, J., Planelles, V., Willey, C., Cron, R. Q., and Kutsch, O. (2014) Kinase Control of Latent HIV-1 Infection: PIM-1 Kinase as a Major Contributor to HIV-1 Reactivation. *J. Virol.* **88**, 364–376
51. Extracellular vesicles: an introduction | Abcam [online] https://www.abcam.com/primary-antibodies/extracellular-vesicles-an-introduction (Accessed July 7, 2022)
52. Gurung, S., Perocheau, D., Touramanidou, L., and Baruteau, J. (2021) The exosome journey: from biogenesis to uptake and intracellular signalling. *Cell Commun. Signal.* **19**, 47
53. Belli, S., Esposito, D., Servetto, A., Pesapane, A., Formisano, L., and Bianco, R. (2020) c-Src and EGFR Inhibition in Molecular Cancer Therapy: What Else Can We Improve? *Cancers*. **12**, 1489
54. Sato, K., Sato, A., Aoto, M., and Fukami, Y. (1995) c-Src phosphorylates epidermal growth factor receptor on tyrosine 845. *Biochem. Biophys. Res. Commun.* **215**, 1078–1087
55. Bao, J., Gur, G., and Yarden, Y. (2003) Src promotes destruction of c-Cbl: Implications for oncogenic synergy between Src and growth factor receptors. *Proc. Natl. Acad. Sci.* **100**, 2438–2443
56. Dienstmann, R., Rodon, J., Serra, V., and Tabernero, J. (2014) Picking the point of inhibition: a comparative review of PI3K/AKT/mTOR pathway inhibitors. *Mol. Cancer Ther.* **13**, 1021–1031
57. Martini, M., De Santis, M. C., Braccini, L., Gulluni, F., and Hirsch, E. (2014) PI3K/AKT signaling pathway and cancer: an updated review. *Ann. Med.* **46**, 372–383
58. Freudlsperger, C., Burnett, J. R., Friedman, J. A., Kannabiran, V. R., Chen, Z., and Van Waes, C. (2011) EGFR-PI3K-AKT-mTOR signaling in head and neck squamous cell carcinomas: attractive targets for molecular-oriented therapy. *Expert Opin. Ther. Targets*. **15**, 63–74
59. Zhou, J., Wulfkuhle, J., Zhang, H., Gu, P., Yang, Y., Deng, J., Margolick, J. B., Liotta, L. A., Petricoin, E., and Zhang, Y. (2007) Activation of the PTEN/mTOR/STAT3 pathway in breast cancer stem-like cells is required for viability and maintenance. *Proc. Natl. Acad. Sci. U. S. A.* **104**, 16158–16163
60. Giraud, S., Bienvenu, F., Avril, S., Gascan, H., Heery, D. M., and Coqueret, O. (2002) Functional interaction of STAT3 transcription factor with the coactivator NcoA/SRC1a. *J. Biol. Chem.* **277**, 8004–8011
61. Walsh, C. A., Qin, L., Tien, J. C.-Y., Young, L. S., and Xu, J. (2012) The Function of Steroid Receptor Coactivator-1 in Normal Tissues and Cancer. *Int. J. Biol. Sci.* **8**, 470–485
62. Lindauer, M., and Hochhaus, A. (2010) Dasatinib. *Recent Results Cancer Res. Fortschritte Krebsforsch. Progres Dans Rech. Sur Cancer*. **184**, 83–102

63. Lindsley, C. W. (2010) The Akt/PKB family of protein kinases: a review of small molecule inhibitors and progress towards target validation: a 2009 update. *Curr. Top. Med. Chem.* **10**, 458–477
64. Li, J., Kim, S. G., and Blenis, J. (2014) Rapamycin: one drug, many effects. *Cell Metab.* **19**, 373–379
65. Wang, Y., Lonard, D. M., Yu, Y., Chow, D.-C., Palzkill, T. G., Wang, J., Qi, R., Matzuk, A. J., Song, X., Madoux, F., Hodder, P., Chase, P., Griffin, P. R., Zhou, S., Liao, L., Xu, J., and O'Malley, B. W. (2014) Bufalin Is a Potent Small-Molecule Inhibitor of the Steroid Receptor Coactivators SRC-3 and SRC-1. *Cancer Res.* **74**, 1506–1517
66. Lu, K., Chen, N., Zhou, X., Ge, X., Feng, L., Li, P., Li, X., Geng, L., and Wang, X. (2015) The STAT3 inhibitor WP1066 synergizes with vorinostat to induce apoptosis of mantle cell lymphoma cells. *Biochem. Biophys. Res. Commun.* **464**, 292–298
67. Parsons, S. J., and Parsons, J. T. (2004) Src family kinases, key regulators of signal transduction. *Oncogene*. **23**, 7906–7909
68. Ingley, E. (2008) Src family kinases: regulation of their activities, levels and identification of new pathways. *Biochim. Biophys. Acta*. **1784**, 56–65
69. Nika, K., Soldani, C., Salek, M., Paster, W., Gray, A., Etzensperger, R., Fugger, L., Polzella, P., Cerundolo, V., Dushek, O., Höfer, T., Viola, A., and Acuto, O. (2010) Constitutively active Lck kinase in T cells drives antigen receptor signal transduction. *Immunity*. **32**, 766–777
70. Palacios, E. H., and Weiss, A. (2004) Function of the Src-family kinases, Lck and Fyn, in T-cell development and activation. *Oncogene*. **23**, 7990–8000
71. McCubrey, J. A., Steelman, L. S., Chappell, W. H., Abrams, S. L., Wong, E. W. T., Chang, F., Lehmann, B., Terrian, D. M., Milella, M., Tafuri, A., Stivala, F., Libra, M., Basecke, J., Evangelisti, C., Martelli, A. M., and Franklin, R. A. (2007) Roles of the Raf/MEK/ERK pathway in cell growth, malignant transformation and drug resistance. *Biochim. Biophys. Acta*. **1773**, 1263–1284
72. Barclay, R. A., Khatkar, P., Mensah, G., DeMarino, C., Chu, J. S. C., Lepene, B., Zhou, W., Gillevet, P., Torkzaban, B., Khalili, K., Liotta, L., and Kashanchi, F. (2019) An Omics Approach to Extracellular Vesicles from HIV-1 Infected Cells. *Cells*. 10.3390/cells8080787
73. Masvekar, R. R., El-Hage, N., Hauser, K. F., and Knapp, P. E. (2015) GSK3β-Activation is a Point of Convergence for HIV-1 and Opiate-Mediated Interactive Neurotoxicity. *Mol. Cell. Neurosci.* **65**, 11–20
74. Kaytor, M. D., and Orr, H. T. (2002) The GSK3 beta signaling cascade and neurodegenerative disease. *Curr. Opin. Neurobiol.* **12**, 275–278
75. Gong, J., Shen, X., Chen, C., Qiu, H., and Yang, R. (2011) Down-regulation of HIV-1 infection by inhibition of the MAPK signaling pathway. *Virol. Sin.* **26**, 114–122
76. Mulcahy, L. A., Pink, R. C., and Carter, D. R. F. (2014) Routes and mechanisms of extracellular vesicle uptake. *J. Extracell. Vesicles*. **3**, 24641

77. Bonsergent, E., Grisard, E., Buchrieser, J., Schwartz, O., Théry, C., and Lavieu, G. (2021) Quantitative characterization of extracellular vesicle uptake and content delivery within mammalian cells. *Nat. Commun.* **12**, 1864
78. Baj-Krzyworzeka, M., Szatanek, R., Weglarczyk, K., Baran, J., Urbanowicz, B., Brański, P., Ratajczak, M. Z., and Zembala, M. (2006) Tumour-derived microvesicles carry several surface determinants and mRNA of tumour cells and transfer some of these determinants to monocytes. *Cancer Immunol. Immunother. CII*. **55**, 808–818
79. Dellar, E. R., Hill, C., Melling, G. E., Carter, D. R. F., and Baena-Lopez, L. A. (2022) Unpacking extracellular vesicles: RNA cargo loading and function. *J. Extracell. Biol.* **1**, e40
80. Skog, J., Würdinger, T., van Rijn, S., Meijer, D. H., Gainche, L., Sena-Esteves, M., Curry, W. T., Carter, B. S., Krichevsky, A. M., and Breakefield, X. O. (2008) Glioblastoma microvesicles transport RNA and proteins that promote tumour growth and provide diagnostic biomarkers. *Nat. Cell Biol.* **10**, 1470–1476
81. Vidal, M. (2019) Exosomes: Revisiting their role as "garbage bags." *Traffic*. **20**, 815–828
82. Andreu, Z., and Yáñez-Mó, M. (2014) Tetraspanins in Extracellular Vesicle Formation and Function. *Front. Immunol.* 10.3389/fimmu.2014.00442
83. Murao, A., Tan, C., Jha, A., Wang, P., and Aziz, M. (2021) Exosome-Mediated eCIRP Release From Macrophages to Induce Inflammation in Sepsis. *Front. Pharmacol.* [online] https://www.frontiersin.org/articles/10.3389/fphar.2021.791648 (Accessed July 13, 2022)
84. Cvjetkovic, A., Jang, S. C., Konečná, B., Höög, J. L., Sihlbom, C., Lässer, C., and Lötvall, J. (2016) Detailed Analysis of Protein Topology of Extracellular Vesicles–Evidence of Unconventional Membrane Protein Orientation. *Sci. Rep.* **6**, 36338
85. Salamango, D. J., Ikeda, T., Moghadasi, S. A., Wang, J., McCann, J. L., Serebrenik, A. A., Ebrahimi, D., Jarvis, M. C., Brown, W. L., and Harris, R. S. (2019) HIV-1 Vif Triggers Cell Cycle Arrest by Degrading Cellular PPP2R5 Phospho-regulators. *Cell Rep.* **29**, 1057-1065.e4
86. DeHart, J. L., Bosque, A., Harris, R. S., and Planelles, V. (2008) Human Immunodeficiency Virus Type 1 Vif Induces Cell Cycle Delay via Recruitment of the Same E3 Ubiquitin Ligase Complex That Targets APOBEC3 Proteins for Degradation. *J. Virol.* **82**, 9265–9272
87. Sakai, K., Barnitz, R. A., Chaigne-Delalande, B., Bidère, N., and Lenardo, M. J. (2011) Human Immunodeficiency Virus Type 1 Vif causes dysfunction of Cdk1 and CyclinB1: implications for cell cycle arrest. *Virol. J.* **8**, 219
88. Zhang, W., Zhong, W., Wang, B., Yang, J., Yang, J., Yu, Z., Qin, Z., Shi, A., Xu, W., Zheng, C., Schuchter, L. M., Karakousis, G. C., Mitchell, T. C., Amaravadi, R., Herlyn, M., Dong, H., Gimotty, P. A., Daaboul, G., Xu, X., and Guo, W. (2022) ICAM-1-mediated adhesion is a prerequisite for exosome-induced T cell suppression. *Dev. Cell*. **57**, 329-343.e7
89. van Niel, G., D'Angelo, G., and Raposo, G. (2018) Shedding light on the cell biology of extracellular vesicles. *Nat. Rev. Mol. Cell Biol.* **19**, 213–228

90. Joshi, B. S., de Beer, M. A., Giepmans, B. N. G., and Zuhorn, I. S. (2020) Endocytosis of Extracellular Vesicles and Release of Their Cargo from Endosomes. *ACS Nano*. **14**, 4444–4455
91. Hill, A. F. (2019) Extracellular Vesicles and Neurodegenerative Diseases. *J. Neurosci.* **39**, 9269–9273
92. Bebelman, M. P., Smit, M. J., Pegtel, D. M., and Baglio, S. R. (2018) Biogenesis and function of extracellular vesicles in cancer. *Pharmacol. Ther.* **188**, 1–11
93. Briaud, P., and Carroll, R. K. (2020) Extracellular Vesicle Biogenesis and Functions in Gram-Positive Bacteria. *Infect. Immun.* **88**, e00433-20
94. Lahiry, P., Torkamani, A., Schork, N. J., and Hegele, R. A. (2010) Kinase mutations in human disease: interpreting genotype–phenotype relationships. *Nat. Rev. Genet.* **11**, 60–74
95. Buljan, M., Ciuffa, R., van Drogen, A., Vichalkovski, A., Mehnert, M., Rosenberger, G., Lee, S., Varjosalo, M., Pernas, L. E., Spegg, V., Snijder, B., Aebersold, R., and Gstaiger, M. (2020) Kinase Interaction Network Expands Functional and Disease Roles of Human Kinases. *Mol. Cell*. **79**, 504-520.e9
96. Kalluri, R., and LeBleu, V. S. (2020) The biology, function, and biomedical applications of exosomes. *Science*. **367**, eaau6977
97. Trible, R. P., Emert-Sedlak, L., and Smithgall, T. E. (2006) HIV-1 Nef Selectively Activates Src Family Kinases Hck, Lyn, and c-Src through Direct SH3 Domain Interaction. *J. Biol. Chem.* **281**, 27029–27038
98. Briggs, S. D., Scholtz, B., Jacque, J. M., Swingler, S., Stevenson, M., and Smithgall, T. E. (2001) HIV-1 Nef promotes survival of myeloid cells by a Stat3-dependent pathway. *J. Biol. Chem.* **276**, 25605–25611
99. Choi, H.-J., and Smithgall, T. E. (2004) HIV-1 Nef promotes survival of TF-1 macrophages by inducing Bcl-XL expression in an extracellular signal-regulated kinase-dependent manner. *J. Biol. Chem.* **279**, 51688–51696
100. Brooks, D. G., Arlen, P. A., Gao, L., Kitchen, C. M. R., and Zack, J. A. (2003) Identification of T cell-signaling pathways that stimulate latent HIV in primary cells. *Proc. Natl. Acad. Sci. U. S. A.* **100**, 12955–12960
101. Strasner, A. B., Natarajan, M., Doman, T., Key, D., August, A., and Henderson, A. J. (2008) The Src Kinase Lck Facilitates Assembly of HIV-1 at the Plasma Membrane. *J. Immunol. Baltim. Md 1950*. **181**, 3706–3713
102. Phipps, D. J., Rhed-Doob, P., Macfadden, D. K., Piovesan, J. P., Mills, G. B., and Branche, D. R. (1995) An octapeptide analogue of HIV gp120 modulates protein tyrosine kinase activity in activated peripheral blood T lymphocytes. *Clin. Exp. Immunol.* **100**, 412–418
103. Phipps, D. J., Yousefi, S., and Branch, D. R. (1997) Increased Enzymatic Activity of the T-Cell Antigen Receptor-Associated Fyn Protein Tyrosine Kinase in Asymptomatic Patients Infected With the Human Immunodeficiency Virus. *Blood*. **90**, 3603–3612
104. Banks, W. A., Sharma, P., Bullock, K. M., Hansen, K. M., Ludwig, N., and Whiteside, T. L. (2020) Transport of Extracellular Vesicles across the Blood-Brain

Barrier: Brain Pharmacokinetics and Effects of Inflammation. *Int. J. Mol. Sci.* **21**, 4407
105. Matsumoto, J., Stewart, T., Banks, W. A., and Zhang, J. (2017) The Transport Mechanism of Extracellular Vesicles at the Blood-Brain Barrier. *Curr. Pharm. Des.* **23**, 6206–6214
106. Wallet, C., De Rovere, M., Van Assche, J., Daouad, F., De Wit, S., Gautier, V., Mallon, P. W. G., Marcello, A., Van Lint, C., Rohr, O., and Schwartz, C. (2019) Microglial Cells: The Main HIV-1 Reservoir in the Brain. *Front. Cell. Infect. Microbiol.* [online] https://www.frontiersin.org/article/10.3389/fcimb.2019.00362 (Accessed January 13, 2022)
107. Ginsberg, S. D., Alldred, M. J., Gunnam, S. M., Schiroli, C., Lee, S. H., Morgello, S., and Fischer, T. (2018) Expression profiling suggests microglial impairment in human immunodeficiency virus neuropathogenesis. *Ann. Neurol.* **83**, 406–417
108. Paplomata, E., and O'Regan, R. (2014) The PI3K/AKT/mTOR pathway in breast cancer: targets, trials and biomarkers. *Ther. Adv. Med. Oncol.* **6**, 154–166
109. Pasquereau, S., and Herbein, G. (2022) CounterAKTing HIV: Toward a "Block and Clear" Strategy? *Front. Cell. Infect. Microbiol.* [online] https://www.frontiersin.org/articles/10.3389/fcimb.2022.827717 (Accessed July 17, 2022)
110. Wolf, D., Witte, V., Laffert, B., Blume, K., Stromer, E., Trapp, S., d'Aloja, P., Schürmann, A., and Baur, A. S. (2001) HIV-1 Nef associated PAK and PI3-Kinases stimulate Akt-independent Bad-phosphorylation to induce anti-apoptotic signals. *Nat. Med.* **7**, 1217–1224
111. Huveneers, S., and Danen, E. H. J. (2009) Adhesion signaling – crosstalk between integrins, Src and Rho. *J. Cell Sci.* **122**, 1059–1069
112. Wu, W., Sun, Z., Wu, J., Peng, X., Gan, H., Zhang, C., Ji, L., Xie, J., Zhu, H., Ren, S., Gu, J., and Zhang, S. (2012) Trihydrophobin 1 Phosphorylation by c-Src Regulates MAPK/ERK Signaling and Cell Migration. *PLOS ONE*. **7**, e29920
113. Yeatman, T. J. (2004) A renaissance for SRC. *Nat. Rev. Cancer*. **4**, 470–480
114. Yang, X., and Gabuzda, D. (1998) Mitogen-activated Protein Kinase Phosphorylates and Regulates the HIV-1 Vif Protein *. *J. Biol. Chem.* **273**, 29879–29887
115. Yang, X., and Gabuzda, D. (1999) Regulation of Human Immunodeficiency Virus Type 1 Infectivity by the ERK Mitogen-Activated Protein Kinase Signaling Pathway. *J. Virol.* **73**, 3460–3466
116. Narayanan, A., Sampey, G., Van Duyne, R., Guendel, I., Kehn-Hall, K., Roman, J., Currer, R., Galons, H., Oumata, N., Joseph, B., Meijer, L., Caputi, M., Nekhai, S., and Kashanchi, F. (2012) Use of ATP analogs to inhibit HIV-1 transcription. *Virology*. **432**, 219–231
117. Sonti, S., Sharma, A. L., and Tyagi, M. (2021) HIV-1 persistence in the CNS: Mechanisms of latency, pathogenesis and an update on eradication strategies. *Virus Res.* **303**, 198523
118. Yang, B., Akhter, S., Chaudhuri, A., and Kanmogne, G. D. (2009) HIV-1 gp120 induces cytokine expression, leukocyte adhesion, and transmigration across the

blood-brain barrier: modulatory effects of STAT1 signaling. *Microvasc. Res.* **77**, 212–219
119. Gazon, H., Barbeau, B., Mesnard, J.-M., and Peloponese, J.-M. (2018) Hijacking of the AP-1 Signaling Pathway during Development of ATL. *Front. Microbiol.* [online] https://www.frontiersin.org/articles/10.3389/fmicb.2017.02686 (Accessed July 20, 2022)
120. Gangnuss, S., Cowin, A. J., Daehn, I. S., Hatzirodos, N., Rothnagel, J. A., Varelias, A., and Rayner, T. E. (2004) Regulation of MAPK activation, AP-1 transcription factor expression and keratinocyte differentiation in wounded fetal skin. *J. Invest. Dermatol.* **122**, 791–804
121. Kilareski, E. M., Shah, S., Nonnemacher, M. R., and Wigdahl, B. (2009) Regulation of HIV-1 transcription in cells of the monocyte-macrophage lineage. *Retrovirology*. **6**, 118
122. Cohen, P., and Frame, S. (2001) The renaissance of GSK3. *Nat. Rev. Mol. Cell Biol.* **2**, 769–776
123. Guendel, I., Iordanskiy, S., Van Duyne, R., Kehn-Hall, K., Saifuddin, M., Das, R., Jaworski, E., Sampey, G. C., Senina, S., Shultz, L., Narayanan, A., Chen, H., Lepene, B., Zeng, C., and Kashanchi, F. (2014) Novel Neuroprotective GSK-3β Inhibitor Restricts Tat-Mediated HIV-1 Replication. *J. Virol.* **88**, 1189–1208
124. Buss, H., Dörrie, A., Schmitz, M. L., Frank, R., Livingstone, M., Resch, K., and Kracht, M. (2004) Phosphorylation of Serine 468 by GSK-3β Negatively Regulates Basal p65 NF-κB Activity *. *J. Biol. Chem.* **279**, 49571–49574
125. Doble, B., and Woodgett, J. R. (2003) GSK-3: tricks of the trade for a multi-tasking kinase. *J. Cell Sci.* **116**, 1175–1186
126. Panagoulias, I., Karagiannis, F., Aggeletopoulou, I., Georgakopoulos, T., Argyropoulos, C. P., Akinosoglou, K., Gogos, C., Skoutelis, A., and Mouzaki, A. (2018) Ets-2 Acts As a Transcriptional Repressor of the Human Immunodeficiency Virus Type 1 through Binding to a Repressor–Activator Target Sequence of 5′-LTR. *Front. Immunol.* [online] https://www.frontiersin.org/articles/10.3389/fimmu.2017.01924 (Accessed July 21, 2022)
127. Goh, W. C., Rogel, M. E., Kinsey, C. M., Michael, S. F., Fultz, P. N., Nowak, M. A., Hahn, B. H., and Emerman, M. (1998) HIV-1 Vpr increases viral expression by manipulation of the cell cycle: A mechanism for selection of Vpr in vivo. *Nat. Med.* **4**, 65–71
128. Wang, J., Reuschel, E. L., Shackelford, J. M., Jeang, L., Shivers, D. K., Diehl, J. A., Yu, X.-F., and Finkel, T. H. (2011) HIV-1 Vif promotes the G1- to S-phase cell-cycle transition. *Blood*. **117**, 1260–1269
129. Anyanwu, S. I., Doherty, A., Powell, M. D., Obialo, C., Huang, M. B., Quarshie, A., Mitchell, C., Bashir, K., and Newman, G. W. (2018) Detection of HIV-1 and Human Proteins in Urinary Extracellular Vesicles from HIV+ Patients. *Adv. Virol.* 10.1155/2018/7863412

130. Jowett, J. B., Planelles, V., Poon, B., Shah, N. P., Chen, M. L., and Chen, I. S. (1995) The human immunodeficiency virus type 1 vpr gene arrests infected T cells in the G2 + M phase of the cell cycle. *J. Virol.* **69**, 6304–6313
131. Wang, J., Shackelford, J. M., Casella, C. R., Shivers, D. K., Rapaport, E. L., Liu, B., Yu, X.-F., and Finkel, T. H. (2007) The Vif Accessory Protein Alters the Cell Cycle of Human Immunodeficiency Virus Type 1 Infected Cells. *Virology*. **359**, 243–252
132. Robert, T., Johnson, J. L., Guichaoua, R., Yaron, T. M., Bach, S., Cantley, L. C., and Colas, P. (2020) Development of a CDK10/CycM in vitro Kinase Screening Assay and Identification of First Small-Molecule Inhibitors. *Front. Chem.* [online] https://www.frontiersin.org/article/10.3389/fchem.2020.00147 (Accessed May 20, 2022)
133. Cohen, P. (2002) Protein kinases — the major drug targets of the twenty-first century? *Nat. Rev. Drug Discov.* **1**, 309–315
134. Biasutto, L., Chiechi, A., Couch, R., Liotta, L. A., and Espina, V. (2013) Retinal pigment epithelium (RPE) exosomes contain signaling phosphoproteins affected by oxidative stress. *Exp. Cell Res.* **319**, 2113–2123
135. Petricoin, E. F., Espina, V., Araujo, R. P., Midura, B., Yeung, C., Wan, X., Eichler, G. S., Johann, D. J., Qualman, S., Tsokos, M., Krishnan, K., Helman, L. J., and Liotta, L. A. (2007) Phosphoprotein pathway mapping: Akt/mammalian target of rapamycin activation is negatively associated with childhood rhabdomyosarcoma survival. *Cancer Res.* **67**, 3431–3440
136. Petricoin, E., Wulfkuhle, J., Howard, M., Pierobon, M., Espina, V., Luchini, A., and Liotta, L. A. (2019) RPPA: Origins, Transition to a Validated Clinical Research Tool, and Next Generations of the Technology. *Adv. Exp. Med. Biol.* **1188**, 1–19

BIOGRAPHY

Gifty A. Mensah is a first-generation college student. She received her Bachelor of Science from George Mason University in 2015. She earned her Master's degree in Biology with a concentration in Microbiology & Infectious Diseases at George Mason University in 2019. Her achievements and the high quality of her research earned her the Graduate Inclusion and Access Scholarship which covered the entirety of her PhD program. Prior to her admission into the Biosciences PhD program, she interned at Inova Fairfax Hospital and worked at Quest Diagnostics where she got her first exposure to clinical laboratory functions and developed a keen interest in the field. During her tenure as a PhD student, she participated in the publication of 6 papers, two of them co-first authored. She has presented her research at local and educational meetings including George Mason's School of Systems Biology Research Day and Graduate Interdisciplinary conferences; as well as national conferences such as the Extracellular Vesicles and Infections conference and the American Society for Exosomes and Microvesicles annual meeting. Additionally, she was a Graduate Teaching Assistant in the undergraduate Microbiology department. Following graduation, Gifty hopes to obtain a postdoctoral fellowship position to further develop her skills and pursue a career as a molecular biologist.